

**NOAA NESDIS
CENTER for SATELLITE APPLICATIONS and
RESEARCH**

**GOES-R Advanced Baseline Imager (ABI)
Algorithm Theoretical Basis Document
For Surface Albedo**

Shunlin Liang, Dongdong Wang, Tao He

University of Maryland

Yunyue Yu, NOAA/NESDIS/STAR

Version 1.0

September 2010

VERSION HISTORY SUMMARY

Version	Description	Revised Sections	Date
0.1	New ATBD Document according to NOAA /NESDIS/STAR Document Guideline		8/30/2008
0.2	GOES-R Advanced Baseline Imager (ABI) Algorithm Theoretical Basis Document for Surface Albedo		9/30/2008
1.0	ATBD Document 80% readiness	Adding discussions on product uses in Section 2; Updating the newly developed algorithm in Section3; Providing validation results in Section 4; Supplementing more details in Sections 5 & 6	6/30/2010

TABLE OF CONTENTS

	<u>Page</u>
LIST OF FIGURES	7
LIST OF TABLES	9
LIST OF ACRONYMS	11
ABSTRACT.....	13
1 INTRODUCTION	15
1.1 Purpose of This Document.....	15
1.2 Who Should Use This Document	15
1.3 Inside Each Section.....	15
1.4 Related Documents	16
1.5 Revision History	16
2 OBSERVING SYSTEM OVERVIEW.....	17
2.1 Products Generated	17
2.2 Instrument Characteristics	18
3 ALGORITHM DESCRIPTION.....	19
3.1 Algorithm Overview	19
3.2 Processing Outline	19
3.3 Algorithm Input	21
3.3.1 Primary Sensor Data	23
3.3.2 Derived Sensor Data	24
3.3.3 Ancillary Data.....	24
3.4 Theoretical Description.....	26
3.4.1 Calculation of BRDF parameters.....	26
3.4.2 Mathematical Description.....	29
3.4.3 Algorithm Output.....	34
4 TEST DATA SETS AND OUTPUTS	41
4.1 Input Data Sets and Ground Measurements.....	41
4.1.1 Proxy Input Data	41
4.1.2 Ground Measurements	43
4.2 Output from Proxy Data.....	44

4.2.1	Output from Simulated Data.....	44
4.2.2	Output from 2D MODIS Data	45
4.2.3	Output from MODIS Data over Field Sites	46
4.2.4	Summary of Estimate Accuracy and Precision.....	50
5	PRACTICAL CONSIDERATIONS.....	53
5.1	Numerical Computation Considerations.....	53
5.2	Programming and Procedural Considerations	53
5.3	Quality Assessment and Diagnostics	53
5.4	Exception Handling	53
5.5	Algorithm Validation.....	54
6	ASSUMPTIONS AND LIMITATIONS	55
6.1	Performance	55
6.2	Assumed Sensor Performance.....	55
6.3	Algorithm Improvement	55
7	REFERENCES	57

LIST OF FIGURES

	<u>Page</u>
Figure 3.1. High level flowchart of the offline mode of ABI LSA algorithm, which is executed once at the end of each day to estimate the BRDF parameters.	20
Figure 3.2. High level flowchart of the online mode of ABI LSA algorithm, illustrating the main processing components.	21
Figure 3.3 ABI products map showing relationships between the ABI LSA product and other ABI data.....	23
Figure 4.1 An example input of AOD time series at the Bondville site. The AODs at 550nm are calculated from AODs at other bands using the Angstrom Equation.	42
Figure 4.2 The retrieved BRDF and the actual BRDF used in the simulation at ABI red and near infrared bands.	45
Figure 4.3 The blacksky albedo maps on May 1st, 2005 around 48.3°N, 102.8°W.	46
Figure 4.4 Comparison between our retrieved albedo and MODIS albedo.....	46
Figure 4.5. Time series of validation results of the LSA algorithm using MODIS as proxy data in 2005 over six SURFRAD sites.	47
Figure 4.6 Scattering plots of our retrieved albedo over SURFRAD	48
Figure 4.7. Time series of validation results of the LSA algorithm using MODIS as proxy data in 2005 over four AmeriFlux sites.....	49
Figure 4.8 Scattering plots of our retrieved albedo over four AmeriFlux sites	50
Figure 4.9 The overall quality of our retrieved albedo and MODIS albedo products using all the four AmeriFlux sites data over year 2005.....	50
Figure 4.10 The overall quality of our retrieved albedo and MODIS albedo products using all the six sites data over year 2005.....	51

LIST OF TABLES

	<u>Page</u>
Table 2.1. GOES-R mission requirements for surface albedo product.	17
Table 2.2. GOES-R mission requirements for surface reflectance product.	17
Table 2.3. Spectral characters of Advanced Baseline Imager	18
Table 3.1. Summary of all inputs for ABI LSA algorithm offline mode.	21
Table 3.2. Summary of all inputs for ABI LSA algorithm online mode.	22
Table 3.3. Input list of primary sensor data.	23
Table 3.4. Input list of derived sensor data.	24
Table 3.5. Entries of LUT.	25
Table 3.6. Input of ancillary data.	25
Table 3.7. Coefficients used to calculate albedo from BRDF parameters.	32
Table 3.8. Outputs of the ABI albedo algorithm offline mode.	34
Table 3.9. Outputs of the ABI albedo algorithm online mode: LSA	35
Table 3.10. Outputs of the ABI albedo algorithm online mode: BRDF	35
Table 3.11. QF definition of ABI intermediate BRDF parameter products	35
Table 3.12. QF definition of ABI LSA products	36
Table 3.13. QF definition of ABI BRDF products	36
Table 3.14. PQI definition of ABI intermediate BRDF parameter products	37
Table 3.15. PQI definition of ABI LSA products	37
Table 3.16. PQI Definition of ABI BRDF products	38
Table 3.17. Metadata of ABI intermediate BRDF parameter products	38
Table 3.18. Metadata of ABI LSA products	38
Table 3.19. Metadata of ABI BRDF products	39
Table 4.1. Comparison of SEVIRI, MODIS and ABI reflective bands.	41
Table 4.2. Detailed information of MODIS test data sets	43
Table 4.3. Information of SURFRAD Stations	44
Table 4.4. Information of AmeriFlux Stations	44
Table 4.5. Information of AmeriFlux Stations	51

LIST OF ACRONYMS

2D	Two Dimension
ABI	Advanced Baseline Imager
ACM	ABI Cloud Mask
AIT	Algorithm Integration Team
AOD	Aerosol Optical Depth
ASTER	Advanced Spaceborne Thermal Emission and Reflection Radiometer
ATBD	Algorithm Theoretical Base Document
AVHRR	Advanced Very High-Resolution Radiometer
BRDF	Bidirectional Reflectance Distribution Function
BRF	Bidirectional Reflectance Factor
ETM+	Enhanced Thematic Mapper Plus
FD	Full Disk
GOES	Geostationary Operational Environmental Satellite
GS-F&PS	Ground Segment Functional and Performance Specification
L1B	Level 1B
LSA	Land Surface Albedo
LUT	Look Up Table
MFRSR	Multi-Filter Rotating Shadowband Radiometers
MISR	Multi-angle Imaging Spectroradiometer
MODIS	Moderate Resolution Imaging Spectroradiometer
MRD	Mission Requirement Document
MSG	Meteosat Second Generation
NCEP	National center for Environmental Prediction
NEDT	Noise Equivalent Delta Temperature
NESDIS	National Environmental Satellite, Data, and Information Service
NOAA	National Oceanic and Atmospheric Administration
PAR	Photosynthetically Active Radiation
POLDER	Polarization and Directionality of the Earth's Reflectance
PQI	Product Quality Information
PSP	Precision Spectral Pyranometer
QF	Quality Flag
QC	Quality Control
SEVIRI	Spanning Enhanced Visible and Infrared Imager
SNR	Signal Noise Ratio
SPOT	Systeme pour l'Observation de la Terre
STAR	Center for Satellite Applications and Research
SURFRAD	SURFace RADIation network
TOA	Top Of Atmosphere
UTC	Coordinated Universal Time
VIIRS	Visible/Infrared Imager /Radiometer Suite

ABSTRACT

This land surface albedo (LSA) Algorithm Theoretical Basis Document (ATBD) provides a high level description and the physical basis for the estimation of LSA with images taken by ABI onboard the Geostationary Environmental Operational Satellite (GOES) R series of NOAA geostationary meteorological satellites. LSA is defined as the ratio between incoming and outgoing irradiance at the earth surface, which is a key component of surface energy budget. Besides five spectral albedos and one broadband shortwave albedo, the LSA algorithm also generates surface reflectance as byproducts. The frequent temporal refreshment, fine spectral resolution and large spatial coverage make ABI a unique data source for mapping LSA. The ABI LSA algorithm combines atmospheric correction and surface BRDF modeling in one optimization step to estimate BRDF parameters for each band. In order to improve computational efficiency, the ABI LSA algorithm is separated into offline mode and online mode. The offline mode is carried out at the end of each day, using a time series of clear-sky observations up to the current day to estimate BRDF parameters for the next days' online mode. In the online mode, LSA and surface reflectance products are produced in real-time. The ABI LSA algorithm has been tested and validated using satellite proxy data and simulated data. Comparison with field measurements shows our algorithm can satisfy the requirements of the GOES-R Ground Segment Functional and Performance Specification (F&PS).

1 INTRODUCTION

The purpose, users, scope, related documents and revision history of this document are briefly described in this section. Section 2 gives an overview of the Advanced Baseline Imager (ABI) Land Surface Albedo (LSA) algorithm derivation objectives and operations concept. Section 3 describes the baseline algorithm, its input data requirements, the theoretical background, mathematical descriptions and output of the algorithm. Some test results will be presented in Section 4. Practical considerations are described in Section 5, and followed by Section 6 on assumptions and limitations. Finally, Section 7 presents the references cited.

1.1 Purpose of This Document

The LSA Algorithm Theoretical Basis Document (ATBD) provides a high level description and the physical basis for the estimation of land surface albedo with images taken by ABI onboard the Geostationary Environmental Operational Satellite (GOES) R series of NOAA geostationary meteorological satellites. The LSA is a key parameter controlling surface radiation and energy budgets. LSA and land surface reflectance are also needed by other algorithms, such as snow coverage and radiation flux products.

1.2 Who Should Use This Document

The intended users of this document are those interested in understanding the physical basis of the algorithms and how to use the output of this algorithm to optimize the albedo estimate for a particular application. This document also provides information useful to anyone maintaining or modifying the original algorithm.

1.3 Inside Each Section

This document is subdivided into the following main sections:

- **System Overview:** Provides relevant details of the ABI and a brief description of the products generated by the algorithm.
- **Algorithm Description:** Provides a detailed description of the algorithm including its physical basis, its input, and its output.
- **Test Data Sets and Output:** Provides a description of the test data sets used to characterize the performance of the algorithm and quality of the data products. It also describes the results from algorithm processing using simulated input data.

- **Practical Considerations:** Provides an overview of the issues involving in numerical computation, programming and procedures, quality assessment and diagnostics and exception handling.
- **Assumptions and Limitations:** Provides an overview of the current limitations of the approach and gives the plan for overcoming these limitations with further algorithm development.

1.4 Related Documents

LSA is one product of ABI product streamlines. The requirements of LSA products can be found in the specifications of the GOES-R Ground Segment Functional and Performance Specification (F&PS). LSA also requires other ABI products as the algorithm input. The readers can refer to these specific ATBDs for more information:

- *GOES-R Algorithm Theoretical Base Document for ABI Aerosol Optical Depth*
- *GOES-R Algorithm Theoretical Base Document for ABI Cloud Mask*
- *GOES-R Algorithm Theoretical Base Document for ABI Downward Shortwave Radiation - Surface*

More references about the algorithm details are given in Section 5.

1.5 Revision History

Version 0.2 of this document was created by Drs. Shunlin Liang and Kaicun Wang of the Department of Geography, University of Maryland, College Park and Dr. Yunyue Yu of NOAA NESDIS, Center for Satellite Applications and Research, Camp Springs, Maryland. According to the reviewers' comments, version of 1.0 was updated by Drs. Shunlin Liang and Dongdong Wang of the Department of Geography, University of Maryland, College Park, and Dr. Yunyue Yu of NOAA.

2 OBSERVING SYSTEM OVERVIEW

This section describes the products generated by the ABI LSA Algorithm and the requirements it places on the sensor.

2.1 Products Generated

This albedo algorithm is responsible for LSA estimation for clear sky pixels identified by the ABI Cloud Mask (ACM) product. Using the ABI Aerosol Optical Depth (AOD) product as the first guess, this algorithm updates AOD and estimates AOD at points where ABI AOD products are not available, and then retrieves the parameters of the land surface Bidirectional Reflectance Distribution Function (BRDF) and derive LSA and land surface reflectance values. It also incorporates albedo climatology from previous satellite products (MODIS) as prior knowledge. Full disk albedos for the solar zenith angle smaller than 70° at five visible and near infrared narrowbands and the shortwave broadband are produced. As a byproduct, full disk surface reflectances at these five bands are generated as well.

The surface albedo/reflectance product requirements defined by the Mission Requirement Document (MRD) and the Ground Segment Functional and Performance Specification (GS-F&PS) (NOAA 2009) are listed in Tables 2.1 and 2.2.

Table 2.1. GOES-R mission requirements for surface albedo product.

Observational Requirement	LEVEL ¹	Geographic Coverage ²	Horiz. Res.	Mapping Accuracy	Msmnt. Range (albedo unit)	Msmnt. Accuracy (albedo unit)	Refresh Rate	Data Latency	Long-term Stability	Extent Qualifier
Albedo: Full Disk	T	FD	2 km	2 km	0 to 1	0.08	60 mins	3236 secs	TBD	LZA <70
	G	C	1 km	0.5 km	0 to 1	0.05			TBD	LZA <70

¹T=target, G=goal

²C=CONUS, FD=full disk, H=hemisphere, M=mesoscale

Table 2.2. GOES-R mission requirements for surface reflectance product.

Observational Requirement	LEVEL ¹	Geographic Coverage ²	Horiz. Res.	Mapping Accuracy	Msmnt. Range	Msmnt. Accuracy	Refresh Rate	Data Latency	Long-term Stability	Extent Qualifier
Reflectance: Full Disk	T	FD	2 km	2 km	0 to 2	0.08	60 mins	3236 secs	TBD	LZA <70
	G	C	1 km	0.5 km	0 to 2	0.05			TBD	LZA <70

¹T=target, G=goal

²C=CONUS, FD=full disk, H=hemisphere, M=mesoscale

As the key component of surface energy budget, satellite albedo products can be used to drive/calibrate/validate climatic, mesoscale atmospheric, hydrological and land surface models. Variation of LSA is also an important indicator of land cover and land use change. Analysis of long-term reliable albedo products will help better understand the human dimension of climate change and how the vegetation-albedo-climate feedbacks work. The land surface reflectance byproducts will be the input to a number of other high-level land surface products, such as the fractional snow cover product.

2.2 Instrument Characteristics

The LSA product is produced from clear-sky pixels observed by the ABI. The final channel set is still being determined as the algorithms are developed and validated. Table 2.3 highlights the ABI channels used by the albedo algorithm.

Table 2.3.Spectral characters of Advanced Baseline Imager

Channel Number	Central Wavelength (μm)	Bandwidth (μm)	Spatial Resolution
1	0.47	0.45 – 0.49	1 km
2	0.64	0.59 – 0.69	0.5 km
3	0.86	0.85– 0.89	1 km
4	1.38	1.37 – 1.39	2 km
5	1.61	1.58 – 1.64	1 km
6	2.26	2.23 – 2.28	2 km
7	3.9	3.80 – 4.00	2 km
8	6.15	5.77 – 6.60	2 km
9	7.0	6.75 – 7.15	2 km
10	7.4	7.24 – 7.44	2 km
11	8.5	8.30 – 8.70	2 km
12	9.7	9.42 – 9.80	2 km
13	10.35	10.10 – 10.60	2 km
14	11.2	10.80 – 11.60	2 km
15	12.3	11.80 – 12.80	2 km
16	13.3	13.00 – 13.60	2 km

Shaded channels are used for Albedo derivation.

3 ALGORITHM DESCRIPTION

This section provides a complete description of the algorithm at the current level of maturity to be improved with each revision.

3.1 Algorithm Overview

Three steps are typically required to estimate the surface albedo from satellite multispectral TOA observations (Liang 2004; Schaaf et al. 2008):

- (1) atmospheric correction,
- (2) surface directional reflectance modeling,
- (3) narrowband-to-broadband conversion.

The typical examples are the MODIS and VIIRS albedo algorithms. The first step converts TOA reflectance into surface directional reflectance, the second step converts directional reflectance into spectral albedos (individual ABI bands), and the last step converts spectral albedos to a broadband albedo. However, this type of method is not suitable for deriving ABI LSA because:

- This method requires the surface reflectance as the input, while the surface reflectance product of ABI will be the byproduct of LSA product.
- The common surface reflectance algorithm requires AOD as the input, while ABI AOD algorithm works only at dark surfaces.

Instead, we propose an optimization method similar to the earlier Meteosat algorithm (Pinty et al. 2000a, b) to directly retrieve surface BRDF parameters, and then use the derived BRDF parameters to calculate LSA and land surface reflectance. A similar strategy was also used to retrieve daily aerosol and surface reflectance simultaneously from the Spinning Enhanced Visible and Infrared Imager (SEVIRI) on the Meteosat Second Generation (MSG) (Govaerts et al. 2010; Wagner et al. 2010). Our proposed algorithm combines atmospheric correction and surface BRDF modeling together in one optimizing code. The optimization process estimates the BRDF parameters by minimizing a cost function considering both TOA reflectance and albedo climatology. Our revision over the previous methods mainly includes:

- AOD can vary over time;
- we use multiple ABI spectral channels enabling accurate production of shortwave broadband albedo;
- we use a different formulation of the atmospheric radiative transfer and surface BRDF model; and
- we incorporate albedo climatology as the constraint of optimization.

3.2 Processing Outline

The retrieval of BRDF parameters needs multiple observations over varied observing geometries. Since ABI is not a multi-angular sensor, we achieve this by using a stack of time series observations over each pixel within a short period time and assume the BRDF parameters stay relatively stable during the compositing period. The organization of time series data and retrieval of BRDF parameters is a time-consuming process. In order to improve the code efficiency, we divide our algorithm into two parts: the offline mode and the online mode. At the end of each day, an offline mode computation is carried out to perform a full inversion of BRDF parameters using the stacked time series data. The calculated BRDF parameters are saved for the usage of the following day's online mode. In the online mode, the pre-calculated BRDF parameters are used to derive full disk LSA and surface reflectance products every 60 minutes. The processing chains of the LSA algorithm offline and online modes are shown in the Figures 3.1 and 3.2, respectively.

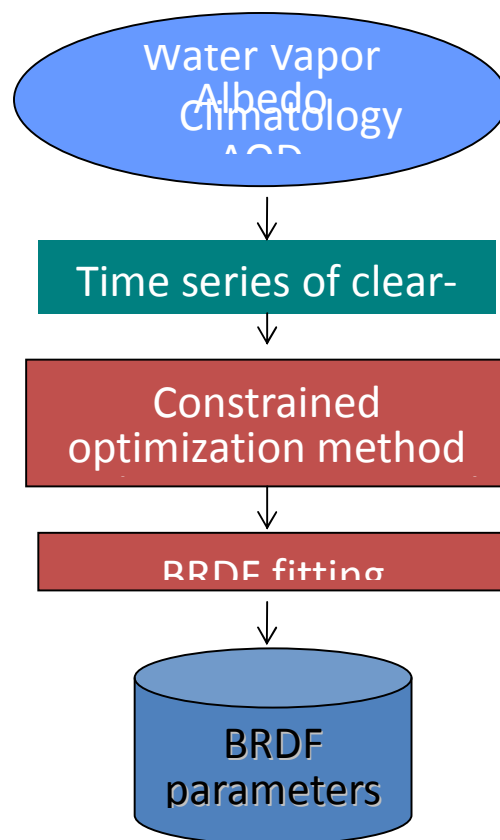


Figure 3.1. High level flowchart of the offline mode of ABI LSA algorithm, which is executed once at the end of each day to estimate the BRDF parameters.

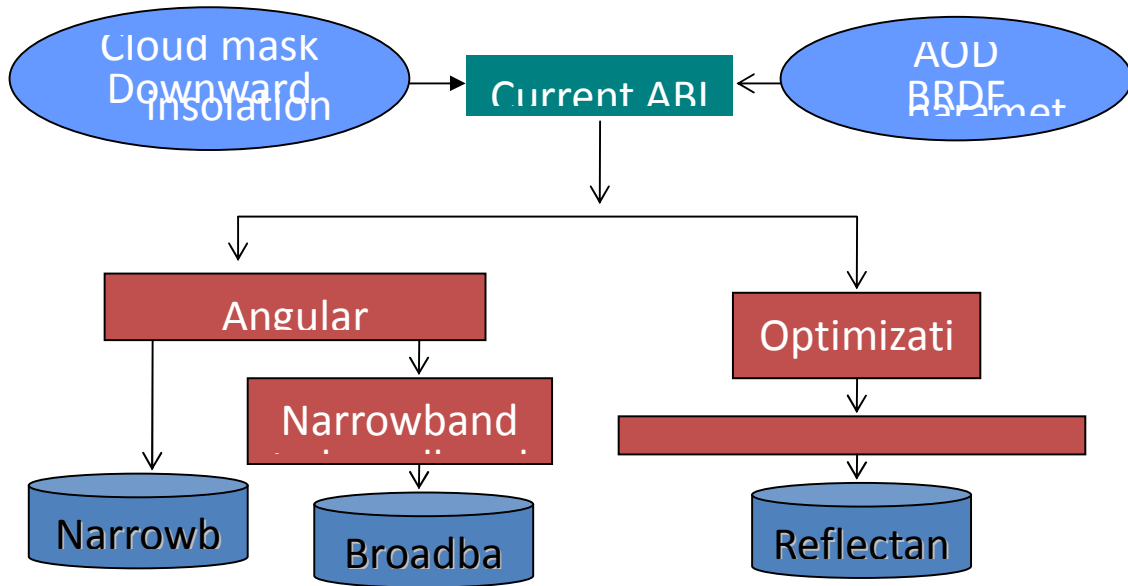


Figure 3.2. High level flowchart of the online mode of ABI LSA algorithm, illustrating the main processing components.

The LSA algorithm will take the ABI AOD product as one input, however, the accuracy and integrity of the AOD product may need to be improved for accurate LSA estimation. For bright surface types or other conditions where the ABI AOD products are not available, the AOD information will be solely obtained from the LSA algorithm. Thus, the ABI AOD products are used as the “first-guess” values. Our strategy is to estimate the land surface BRDF parameters and update AOD information simultaneously based on the initial estimates of AOD and albedo climatologies.

The AOD and other atmospheric parameters (e.g. ozone and water vapor), together with a BRDF model, will facilitate a full inversion of BRDF parameters. After determining the BRDF parameters, the integration over the entire viewing hemisphere produces the spectral albedos, and the downward irradiance values are used for converting spectral albedos to a broadband albedo. Given the BRDF parameters, a full atmospheric correction is then implemented one more time to obtain surface reflectance, without need for the Lambertian surface assumption.

3.3 Algorithm Input

This section describes the input required to execute the LSA algorithm. The offline mode and online mode have different requirements. Tables 3.1 and 3.2 list them, respectively. Figure 3.3 shows the relationship between LSA and other ABI data.

Table 3.1. Summary of all inputs for ABI LSA algorithm offline mode.

Sensor input	TOA reflectance at five bands
--------------	-------------------------------

(Two weeks' time series)		Viewing zenith angle
		Solar zenith angle
		Relative azimuth angle
		Geolocation
		Level 1b Quality Control (QC) flags
Ancillary data (Time series)	ABI data	Aerosol optical depth and aerosol type
		Cloud mask
	Non-ABI static data	Surface albedo climatology
		LUT
		Land/ocean mask
	Non-ABI dynamic data	Water vapor content

Table 3.2. Summary of all inputs for ABI LSA algorithm online mode.

Sensor input		TOA reflectance at five bands
		Viewing zenith angle
		Solar zenith angle
		Relative azimuth angle
		Geolocation
		Level 1b QC flags
Ancillary data	ABI data	Aerosol optical depth
		Downward shortwave radiation(DSR) - surface
		Cloud mask
	Non-ABI static data	Surface albedo climatology
		LUT
	Non-ABI dynamic data	Land/ocean mask
		Pre-calculated BRDF parameters
		Water vapor content

Basically, the offline mode algorithm needs time series of all types of input data and the online mode involves only the data sets at the current observation time. Different from the offline mode, the online mode needs the downward shortwave radiation to calculate the ratio of diffuse radiation. Accordingly, the online mode needs the pre-calculated BRDF parameters as the input. For one particular data set, the online mode and offline mode share the same data details, which are given in the following subsections.

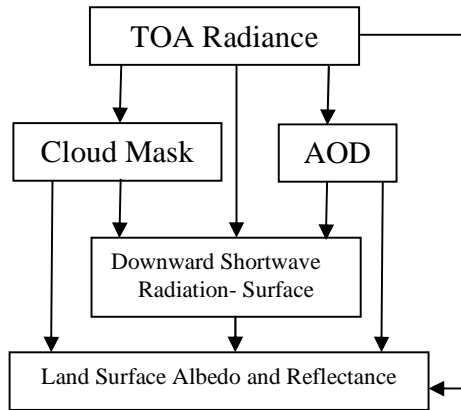


Figure 3.3 ABI products map showing relationships between the ABI LSA product and other ABI data

3.3.1 Primary Sensor Data

Primary sensor data is information that is derived solely from the ABI observations. The primary sensor data used by the LSA algorithm include both the TOA radiance values and relevant ancillary information (angles, geolocation and data quality).

Table 3.3. Input list of primary sensor data.

Name	Type	Description	Dimension
Ch1	input	Calibrated ABI level 1b radiance at channel 1	grid (xsize, ysize)
Ch2	input	Calibrated ABI level 1b radiance at channel 2	grid (xsize, ysize)
Ch3	input	Calibrated ABI level 1b radiance at channel 3	grid (xsize, ysize)
Ch5	input	Calibrated ABI level 1b radiance at channel 5	grid (xsize, ysize)
Ch6	input	Calibrated ABI level 1b radiance at channel 6	grid (xsize, ysize)
Latitude	input	Pixel latitude	grid (xsize, ysize)
Longitude	input	Pixel longitude	grid (xsize, ysize)
Solar zenith	input	ABI solar zenith angles	grid (xsize, ysize)
Solar azimuth	input	ABI solar azimuth angles	grid (xsize, ysize)
View zenith	input	ABI view zenith angle	grid (xsize, ysize)
View azimuth	input	ABI view azimuth angle	grid (xsize, ysize)
QC flags	input	ABI quality control flags with level 1b data	grid (xsize, ysize)

3.3.2 Derived Sensor Data

There are three ABI derived sensor data products required by the LSA algorithm: 1) the ABI Cloud Mask (ACM) product, which indicates four cloudiness states for each pixel: clear, probably clear, probably cloudy, and cloudy, and 2) the ABI AOD product and 3) the ABI Downward Shortwave Radiation – Surface (DSR) product.

Table 3.4. Input list of derived sensor data.

Name	Type	Description	Dimension
Cloud mask	input	ABI cloud mask product	grid (xsize, ysize)
AOD	input	ABI AOD product	grid (xsize, ysize)
DSR	input	ABI DSR product	grid (xsize, ysize)

3.3.3 Ancillary Data

Ancillary data are data other than the ABI sensor and derived data (Table 3.6). The following lists and briefly describes the ancillary data required to run the LSA algorithm.

- **Land/water mask**
The ABI LSA products are generated over land pixels only. Land/water mask is used to mask water pixel.
- **Water vapor content**
The atmospheric water content information is used for atmospheric corrections and the coefficients stratification of the algorithm. If such information is not available from the ABI derived sensor data, the NCEP 6-hour forecasting data will be applied.
- **LSA Climatology**
The albedo climatology includes the mean and variance of land surface spectral and broadband albedos. The albedo climatology will be used as the background values in the albedo estimation. Multiple years' MODIS albedo products are averaged and used as climatology.
- **Look-Up table**
In order to improve the computational efficiency, the atmospheric parameters have been pre-calculated using the 6S simulation and stored into the look-up table (LUT). LUT is a type of static input to the algorithm and all codes share the same set of LUT. The parameters in the LUT include:
 - Atmospheric intrinsic reflectance
 - Total global gas transmittance
 - Downward total scattering transmittance

- Upward total scattering transmittance
- Total spherical albedo
- Optical depth
- Direct irradiance ratio

After a sensitivity analysis, we select the entries of our LUT by balancing the accuracy and the computational efficiency (Table 3.5).

Table 3.5 Entries of LUT.

Entries to LUT	Values
Solar Zenith Angle	0.,5.,10.,15.,20.,25.,30.,35.,40.,45.,50.,55.,60.,65.,70.,75., 80.
Sensor Zenith Angle	0.,5.,10.,15.,20.,25.,30.,35.,40.,45.,50.,55.,60.,65.,70.,75., 80.
Relative Azimuth Angle	0.,10.,20.,30.,40.,50.,60.,70.,80.,90.,100.,110., 120.,130.,140.,150.,160.,170.,180.
Aerosol Optical Depth	.01,.05,.1.,15.,2.,3.,4.,6.,8.,1.,1.5,2.,3.,4.

- **BRDF parameters**

BRDF parameters are useful for integrating albedo and correcting surface reflectance. The parameters are the output of the offline mode code and also the input of the online mode code.

Table 3.6 Input of ancillary data.

Name	Type	Description	Dimension
Land/water mask	input	A land-water mask	grid (xsize, ysize)
Water vapor	input	NCEP water vapor 6-hour forecast data	grid (xsize, ysize)
Albedo climatology	input	MODIS multiple years' mean	grid (xsize, ysize)
Atmosphere LUT	input	Seven atmospheric parameters as function of aerosol model, aerosol optical depth, ABI channel and observing geometry	(17x 17 x 19 x 14 x 5)*
Ch1 f_iso	input	BRDF isotropic component parameter at Ch1	grid (xsize, ysize)
Ch1 f_vol	input	BRDF volumetric kernel parameter at Ch1	grid (xsize, ysize)
Ch1 f_geo	input	BRDF geometric kernel parameter at Ch1	grid (xsize, ysize)
Ch2 f_iso	input	BRDF isotropic component parameter at Ch2	grid (xsize, ysize)
Ch2 f_vol	input	BRDF volumetric kernel parameter at Ch2	grid (xsize, ysize)
Ch2 f_geo	input	BRDF geometric kernel parameter at Ch2	grid (xsize, ysize)
Ch3 f_iso	input	BRDF isotropic component parameter at Ch3	grid (xsize, ysize)
Ch3 f_vol	input	BRDF volumetric kernel parameter at Ch3	grid (xsize, ysize)
Ch3 f_geo	input	BRDF geometric kernel parameter at Ch3	grid (xsize, ysize)
Ch5 f_iso	input	BRDF isotropic component parameter at Ch5	grid (xsize, ysize)
Ch5 f_vol	input	BRDF volumetric kernel parameter at Ch5	grid (xsize, ysize)
Ch5 f_geo	input	BRDF geometric kernel parameter at Ch5	grid (xsize, ysize)

Ch6 f_iso	input	BRDF isotropic component parameter at Ch6	grid (xsize, ysize)
Ch6 f_vol	input	BRDF volumetric kernel parameter at Ch6	grid (xsize, ysize)
Ch6 f_geo	input	BRDF geometric kernel parameter at Ch6	grid (xsize, ysize)

* num_solar_zenith_angle * num_sensor_senith_angle * num_relative_azimuth_angle *
num_aerosol_optical_depth * num_bands

3.4 Theoretical Description

After analyzing existing albedo algorithms, we proposed an ABI LSA algorithm similar to the earlier Meteosat (Pinty et al. 2000a, b) and MSG/SEVIRI approach (Govaerts et al. 2010; Wagner et al. 2010). The albedo algorithm from the geostationary Meteosat observations combined atmospheric correction and BRDF fitting by assuming one unknown constant AOD for the whole period of time (daily). Here, we made several major revisions. For example, AOD can vary over time, and multiple ABI spectral bands enable production of multiple broadband albedos. In addition, the formulation of the atmospheric radiative transfer and surface directional reflectance model are also different. Typically, our algorithm includes the following four steps:

1. Deriving BRDF parameters. We directly obtain BRDF by minimizing the cost function considering both prior knowledge and observations.
2. Calculating spectral albedo, involving angular integration of surface reflectance
3. Converting narrowband albedos to broadband albedo
4. Correcting surface reflectance by considering BRDF. This surface reflectance will be used as the surface reflectance product.

3.4.1 Calculation of BRDF parameters

The critical step of retrieving LSA and land surface reflectance is to estimate the surface BRDF parameters. In order to obtain these parameters, we need to carry out the atmospheric correction and BRDF fitting. A traditional way (e.g. the MODIS albedo algorithm) to achieve this is to implement them separately in two steps. Here, we achieve this in one step by combining both the atmospheric radiative transfer process and BRDF modeling in our optimization schema. The albedo climatology is also used as a constraint of optimization.

3.4.1.1 Atmospheric correction

Atmospheric effects include molecular and aerosol scattering and absorption by gases, such as water vapor, ozone, oxygen and aerosols. Molecular scattering and absorption by ozone and oxygen are relatively easy to correct because their concentrations are stable over both time and space. Because the effect of water vapor absorption is significant, we will use ABI water vapor retrieval (or the NCEP 6-hour forecasting data) to correct the water vapor effect on ABI observations. The most difficult component of atmospheric correction is to eliminate the effects of aerosols, which requires accurate information on

the spatial distribution of aerosol properties that have to be estimated from satellite observations.

There is a relatively long history of the quantitative estimation of AOD from remotely sensed imagery (Liang 2004) using multiangular information (Diner et al. 2005; North 2002) polarization information (Deuze et al. 2001), multispectral information (Kaufman et al. 1997; Liang et al. 1997) and multitemporal information (Christopher et al. 2002; Hauser et al. 2005). The MODIS science team (Kaufman et al. 1997; Remer et al. 2005) uses the dark-object method to estimate AOD from MODIS imagery over land for climate study. However, its major limitation is its suitability only for densely vegetated (“dark”) surfaces. If no dense vegetation canopies are detected in a defined area (e.g., 10 km x 10 km for MODIS), no aerosol retrieval occurs. In our recent study (Liang et al. 2006), we proposed a method using multitemporal information of MODIS data. The validation results (Zhong et al. 2007) indicated our algorithm is very effective.

AOD is a standard product of GOES-R ABI data streamline. However, the accuracy and integrity of the ABI aerosol product may be insufficient to calculate LSA. Our strategy is to apply the ABI aerosol product as the “first-guess” value. We then use an optimization approach to improve the aerosol estimate and to estimate the BRDF parameters simultaneously. If the ABI aerosol product is evaluated as very accurate, we will mainly focus on estimating the surface BRDF parameters. We consider this procedure as a further adjustment of AOD product for better determination of surface reflectance anisotropy, rather than a completely new atmospheric correction procedure. To speed-up the process, the atmospheric parameters are precalculated and stored in LUTs.

3.4.1.2 Land surface BRDF model

Performance of albedo retrieval from satellite observations is usually restricted by a limited sampling of directional surface reflectance. Therefore, a model is usually used to characterize the surface anisotropy. The model can be inverted with a finite set of angular samples and used to calculate surface reflectance in any sun-view geometry and to derive surface albedo. An empirical kernel-based BRDF model will be used in the ABI LSA algorithm.

Maignan et al. (2004) found that among the current directional reflectance models, the best two are the three-parameter linear Ross–Li model and the nonlinear Rahman–Pinty–Verstraete model. However, all models fail to accurately reproduce the sharp reflectance increase close to the backscattering (hotspot peak) direction. Based on physical considerations, Maignan et al. (2004) suggested a modification of the Ross–Li model, without the addition of a free parameter, to account for the complex radiative transfer within the land surfaces that leads to the hot spot signature. They illustrated that the modified linear model performs better than all others.

This modified Ross-Li model will be used in the LSA algorithm and the mathematic details of this model will be given in Section 3.5.1.

3.4.1.3 Land surface albedo climatology

One of the most important features of our ABI LSA algorithm is the use of existing albedo products as the prior knowledge. Many satellite data including AVHRR, MODIS, MISR, GOES are used for generating albedo products. They may have different spatial and temporal resolutions and coverage, but all provides primary knowledge on surface albedo. We intend to integrate these products using data fusion techniques and to generate climatology (mean and variation). If the variation or uncertainty matrix of the albedo climatology is small at the given space and time, our albedo algorithm estimates albedo based mainly on the mean value of the previous products. Otherwise, it relies primarily on ABI observations.

In the original satellite albedo product, there are many “gaps” due to cloud cover and other retrieval failure. NASA has funded a number of our studies that potentially will contribute to an improved albedo climatology. We have developed a spatial-temporal filtering technique to fill the gaps within MODIS albedo products (Fang et al. 2007). We have also explored different data fusion methods that can integrate albedo from different satellite products, such as the Optimal Interpolation (Wang and Liang 2010a), Empirical Orthogonal Function (Wang and Liang 2010b), multiresolution tree (Wang and Liang 2010c) and others.

3.4.1.4 Calculation of spectral albedos

After obtaining BRDF parameters, it is straightforward to calculate spectral albedos, which are simply integrations of the surface directional reflectance functions over the entire viewing hemisphere. The spectral albedos are denoted as narrowband albedos in the next section. Instead of directly carrying out the numeric integration, we calculate the integral using an empirical polynomial equation of the three kernel parameters, similar to the MODIS albedo algorithm (Schaaf et al. 2002). The details are given in Section 3.5.4.

3.4.1.5 Narrowband to broadband conversion

After the narrowband albedos are obtained from the integration of the directional reflectance model, narrowband to broadband conversions are carried out based on empirical statistical relationships. The broadband albedo mainly depends on surface spectral albedo spectra, but is also affected by the atmospheric conditions. With extensive radiative transfer simulations and surface reflectance spectral measurements, we have developed the conversion formulas for calculating the total shortwave albedo, total-, direct-, and diffuse-, visible, and near-infrared broadband albedos for several narrowband sensors (Liang 2001; Liang et al. 2003), including ASTER, AVHRR, GOES, Landsat-7 ETM+, MISR, MODIS, POLDER, and VEGETATION in SPOT spacecraft. A similar approach was later applied to generate the conversion formula for VIIRS (Liang et al. 2005a). The formula for MODIS has been used for routine albedo production (Schaaf et al. 2002), the MISR formula for calculating shortwave albedo is very effective (Chen et al. 2008), and the VIIRS formula will be used for operational albedo production. The

same strategy also will be used to convert five ABI narrowband albedos to one broadband albedo.

3.4.1.6 Derivation of surface reflectance

Traditional atmospheric correction does not account for the surface BRDF effect. The surface reflectance products derived from this type of methods are based on the assumption that the surface is Lambertian (e.g. MODIS surface reflectance product (Vermote et al. 2002)). As the byproduct of ABI LSA, our ABI land surface reflectance products will take full advantage of BRDF information gathered in the process of retrieving albedo. We calculate the surface reflectance from the Qin et al. (2001)'s equation by considering the coupled BRDF effects between the surface and the atmosphere. The BRDF parameters from the offline mode and ABI AOD when applicable will be the input of our surface reflectance algorithm.

3.4.2 Mathematical Description

This subsection gives the mathematical details of the steps above mentioned.

3.4.2.1 Land surface BRDF model

A simple linear model is adopted to represent the surface BRDF. The modified three-parameter linear Ross–Li BRDF model can be written as (Maignan et al. 2004):

$$r_{dd}(\theta_s, \theta_v, \phi) = f_{iso} + f_{vol} \cdot K_{vol}(\theta_s, \theta_v, \phi) + f_{geo} \cdot K_{geo}(\theta_s, \theta_v, \phi) \quad (1)$$

where the volumetric and geometrical kernel function has the following form:

$$K_{vol} = \frac{(\pi/2 - \xi) \cos \xi + \sin \xi}{\cos \theta_s + \cos \theta_v} \left(1 + \frac{1}{1 + \frac{\xi}{\xi_0}} \right) - \frac{\pi}{4} \quad (2)$$

$$K_{geo} = O(\theta_s, \theta_v, \phi) - \sec \theta_s - \sec \theta_v + 0.5(1 + \cos \xi) \sec \theta_s \sec \theta_v \quad (3)$$

and where

$$O = (t - \sin t \cos t)(\sec \theta_s + \sec \theta_v) / \pi \quad (4)$$

$$\cos t = \frac{h\sqrt{D^2 + (\tan \theta_s \tan \theta_v \sin \phi)^2}}{b(\sec \theta_s + \sec \theta_v)} \quad (5)$$

$$D = \sqrt{\tan^2 \theta_s + \tan^2 \theta_v - 2 \tan \theta_s \tan \theta_v \cos \phi} \quad (6)$$

$$\cos \xi = \cos \theta_s \cos \theta_v + \sin \theta_s \sin \theta_v \cos \phi \quad (7)$$

and where $\xi_0=0.026$, $\frac{h}{b}=2.0$, and all the angles have the unit of radian.

3.4.2.2 Formulation of TOA reflectance

To retrieve AOD and the parameters of the surface BRDF from TOA reflectance, we have to establish TOA reflectance as a function of BRDF and AOD. Here, we use the formulation proposed by Qin et al. (2001). The formula for TOA BRF $\rho(\Omega_s, \Omega_v)$ is expressed as:

$$\rho(\Omega_s, \Omega_v) = \rho_0(\Omega_s, \Omega_v) + \frac{T(\Omega_s)R(\Omega_s, \Omega_v)T(\Omega_v) - t_{dd}(\Omega_s)t_{dd}(\Omega_v)|R(\Omega_s, \Omega_v)|\bar{\rho}}{1 - r_{hh}\bar{\rho}} \quad (8)$$

where $\Omega_s \in (-\mu_s, \phi_s)$ is the solar incoming direction, and $\Omega_v \in (\mu_v, \phi_v)$ for the viewing direction. There are two groups of coefficients in the above expression that are independent of each other: atmosphere-dependent and surface-dependent. These coefficients in each group represent the inherent properties of either the atmosphere or the surface. This means that we can determine these two groups of coefficients separately.

For the atmosphere, $\rho_0(\Omega_s, \Omega_v)$ is the atmospheric reflectance associated with path radiance (zero surface reflectance), and $\bar{\rho}$ is the atmospheric spherical albedo as defined before. The transmittance matrices are defined as:

$$T(\Omega_s) = [t_{dd}(\Omega_s) \quad t_{dh}(\Omega_s)] \quad (9)$$

$$T(\Omega_v) = [t_{dd}(\Omega_v) \quad t_{hd}(\Omega_v)]^T \quad (10)$$

where the subscript T stands for transpose, each transmittance has two subscript symbols: d (directional) and h (hemispherical).

The direct transmittance (t_{dd}) has the simple analytical expression: $t_{dd}(\mu) = \exp(-\tau_t / \mu)$.

The directional-hemispheric transmittance (t_{dh}) defines the fraction of downward diffuse flux generated by atmospheric scattering as the direct beam passes through the atmosphere. It can be calculated as the ratio of the integrated sky radiance at the surface level $L^\downarrow(\Omega_s, \Omega_v)$ over the downward hemisphere to the TOA incoming solar radiation:

$$t_{dh}(\Omega_s) = \frac{\int_{2\pi^-} L^\downarrow(\Omega_s, \Omega_v) \mu_v d\Omega_v}{\mu_s F_0} \quad (11)$$

The hemispheric-directional transmittance (t_{hd}) is defined as the ratio of the integrated upwelling TOA radiance over the upper hemisphere to the upwelling flux at the surface level F^\uparrow :

$$t_{hd}(\Omega_v) = \frac{\int_{2\pi^+} L^\uparrow(\Omega_s, \Omega_v) \mu_s d\Omega_s}{F^\uparrow}. \quad (12)$$

where both t_{dh} and t_{hd} have to be calculated numerically. A practical solution is to create look-up tables in advance.

For the surface, the reflectance matrix is defined as:

$$R(\Omega_s, \Omega_v) = \begin{bmatrix} r_{dd}(\Omega_s, \Omega_v) & r_{dh}(\Omega_s) \\ r_{hd}(\Omega_v) & r_{hh} \end{bmatrix} \quad (13)$$

where $r_{dd}(\Omega_s, \Omega_v)$ is bi-directional reflectance and equivalent to the Bidirectional Reflectance Factor (BRF) defined by Eq. (1). The directional-hemispherical reflectance ($r_{dh}(\Omega_s)$) (or black-sky albedo) is defined as:

$$r_{dh}(\Omega_s) = \frac{1}{\pi} \int_{2\pi^+} r_{dd}(\Omega_s, \Omega_v) d\Omega_v, \quad (14)$$

where the integration is over the upper hemisphere. The hemispherical-directional reflectance ($r_{hd}(\Omega_v)$) (or white-sky albedo) is defined in the same way, but the integration is over the lower hemisphere:

$$r_{hd}(\Omega_v) = \frac{1}{\pi} \int_{2\pi^-} r_{dd}(\Omega_s, \Omega_v) d\Omega_s \quad (15)$$

The bi-hemispherical reflectance (r_{hh}) is:

$$r_{hh} = 2 \int_0^1 r_{dh}(\mu_s) \mu_s d\mu_s \quad (16)$$

where $\mu_s = \cos(\theta_s)$.

The determinant $|R|$ is easily calculated as:

$$|R(\Omega_s, \Omega_v)| = r_{dd}(\Omega_s, \Omega_v) r_{hh} - r_{dh}(\Omega_s) r_{hd}(\Omega_v) \quad (17)$$

It is evident that as long as surface BRDF is known, the surface reflectance matrix can be determined. The authors claim that this approach does not introduce any approximation into the formulation, and their numerical experiments demonstrate that this formulation is very accurate (Qin et al., 2001).

3.4.2.3 Determination of AOD and BRDF parameters

Given the surface BRDF model (1) and the atmospheric radiative transfer model (8), the three BRDF parameters and AOD at each observation can be obtained by minimizing the following cost function:

$$J(x) = (r(x) - r_b)B^{-1}(r(x) - r_b) + (\hat{\rho}(x) - \rho)R^{-1}(\hat{\rho}(x) - \rho) + J_c = J_b + J_o + J_c \quad (18)$$

Where x are the three coefficients of the surface BRDF model and AOD, $r(x)$ is the calculated surface albedo using the BRDF model (1), r_b are the "first-guess" values of albedo from albedo climatology (see Section 3.4.1.3), B is the uncertainty matrix of the albedo "first-guess" values, ρ is the observed ABI TOA reflectance, $\hat{\rho}$ is the calculated TOA reflectance from equation (8), and R is the error matrix of the calculated TOA reflectance. J_c is the cost function to account for various constrains, J_b is the cost function of the background, and J_o is the cost function of the ABI data fitting.

If the ABI AOD product is accurate, we estimate only three coefficients of the surface BRDF model. The optimization process is then much simpler. If the accurate AOD is not available, we will estimate AOD and the BRDF parameters simultaneously.

There are many different approaches available for minimizing the cost function. We employ the Shuffled Complex Evolution method (SCE-UA, Duan et al. (1992) and Duan et al. (1993)), an efficient algorithm in searching global optimals. The SCE-UA method is capable of handling high parameter dimensionality and it does not rely on the availability of an explicit expression for the objective function or the derivatives.

3.4.2.4 Calculation of spectral albedo

An angular integration over all the viewing angles is required to calculate albedo from BRDF parameters. Instead of directly calculating the integral, we use a similar method to MODIS (Schaaf et al. 2002), fitting blacksky albedo with a polynomial function:

$$\alpha_{bs}(\theta_s) = f_{iso}a + f_{vol}(b_0 + b_1\theta_s + b_2\theta_s^2 + b_3\theta_s^3) + f_{geo}(c_0 + c_1\theta_s + c_2\theta_s^2 + c_3\theta_s^3) \quad (19)$$

Where θ_s is solar zenith angle, and $a_0, a_1, a_2, b_0, b_1, b_2, c_0, c_1, c_2$ are the regression coefficients, whose values are listed in Table 3.7. Similarly, the whitesky albedo can be computed by using the equation:

$$\alpha_{ws} = f_{iso}a + f_{vol}b + f_{geo}c \quad (20)$$

Table 3.7. Coefficients used to calculate albedo from BRDF parameters.

Variable	Value
a	1.0
b ₀	-0.0374

b ₁	0.5699
b ₂	-1.1252
b ₃	0.8432
c ₀	-1.2665
c ₁	-0.1662
c ₂	0.1829
c ₃	-0.1489
a	1.0
b	0.2260
c	-1.3763

3.4.2.5 Calculation of all sky albedo

Using the equation (19) and (20), we can obtain both black-sky and white-sky albedo. Given the black-sky and white-sky albedo, the all-sky albedo α can be calculated by:

$$\alpha = p\alpha_{ws} + (1 - p)\alpha_{bs} \quad (21)$$

where p is the diffuse fraction of the total radiation. p can be obtained through its empirical relationship with the ratio k of total insolation to extraterrestrial solar radiation (Orgill and Hollands 1977):

$$p = \begin{cases} 1.577 - 1.84k, 0.35 \leq k \leq 0.75 \\ 1 - 0.249k, k < 0.35 \\ 0.177, k > 0.75 \end{cases} \quad (22)$$

The insolation can be obtained from ABI DSR product and the extraterrestrial solar radiation E_0 can be easily calculated from the solar constant c:

$$E_0 = c \cos \theta_s \quad (23)$$

where θ_s is solar zenith angel.

3.4.2.6 Calculation of broadband albedo

The broadband albedo can be converted from spectral albedos using the following empirical formula:

$$\bar{r}(\theta_s) = \beta_0 + \beta_1 F_1 r_1(\theta_s) + \beta_2 F_2 r_2(\theta_s) + \beta_3 F_3 r_3(\theta_s) + \beta_5 F_5 r_5(\theta_s) + \beta_6 F_6 r_6(\theta_s) \quad (24)$$

where $r_i(\theta_s)$ are the spectral albedo, β_i are the coefficients, F_i are the normalized downward irradiance of the ABI five bands:

$$F_i = \frac{E_i(\theta_s)}{E_1(\theta_s) + E_2(\theta_s) + E_3(\theta_s) + E_5(\theta_s) + E_{6i}(\theta_s)} \quad (25)$$

and $E_i(\theta_s)$ are the downward irradiance of each band (at the specific solar zenith angle). Radiative transfer simulations and statistical analysis provide the coefficients β_i .

3.4.3 Algorithm Output

The outputs of the LSA algorithm offline mode mainly include the three parameters of the BRDF model for each ABI band (Table 3.8), which will be used as one input of the online mode. The final outputs of the LSA algorithm online mode are instantaneous albedos and reflectances. These albedo values and description of their meaning are given in Table 3.9. BRF at five bands are also produced as the by-products of LSA. However, the availability and quality of albedo and reflectance products are slightly different due to the difference between their theoretical algorithm bases. Accordingly, the BRF products are organized in separate files (Table 3.10).

Table 3.8. Outputs of the ABI albedo algorithm offline mode.

Name	Type	Description	Dimension
Ch1 f_iso	float	BRDF isotropic component parameter at Ch1	grid (xsize, ysize)
Ch1 f_vol	float	BRDF volumetric kernel parameter at Ch1	grid (xsize, ysize)
Ch1 f_geo	float	BRDF geometric kernel parameter at Ch1	grid (xsize, ysize)
Ch2 f_iso	float	BRDF isotropic component parameter at Ch2	grid (xsize, ysize)
Ch2 f_vol	float	BRDF volumetric kernel parameter at Ch2	grid (xsize, ysize)
Ch2 f_geo	float	BRDF geometric kernel parameter at Ch2	grid (xsize, ysize)
Ch3 f_iso	float	BRDF isotropic component parameter at Ch3	grid (xsize, ysize)
Ch3 f_vol	float	BRDF volumetric kernel parameter at Ch3	grid (xsize, ysize)
Ch3 f_geo	float	BRDF geometric kernel parameter at Ch3	grid (xsize, ysize)
Ch5 f_iso	float	BRDF isotropic component parameter at Ch5	grid (xsize, ysize)
Ch5 f_vol	float	BRDF volumetric kernel parameter at Ch5	grid (xsize, ysize)
Ch5 f_geo	float	BRDF geometric kernel parameter at Ch5	grid (xsize, ysize)
Ch6 f_iso	float	BRDF isotropic component parameter at Ch6	grid (xsize, ysize)
Ch6 f_vol	float	BRDF volumetric kernel parameter at Ch6	grid (xsize, ysize)
Ch6 f_geo	float	BRDF geometric kernel parameter at Ch6	grid (xsize, ysize)
QF	char	Quality flag for each pixel, indicating the general retrieval quality	grid (xsize, ysize)
PQI	char	Quality control flags for each pixel, indicating	grid (xsize, ysize)

		additional BRDF quality	
--	--	-------------------------	--

Table 3.9. Outputs of the ABI albedo algorithm online mode: LSA

Name	Type	Description	Dimension
Ch1 Albedo	float	Derived narrowband albedo value at 0.47 μm	grid (xsize, ysize)
Ch2 Albedo	float	Derived narrowband albedo value at 0.64 μm	grid (xsize, ysize)
Ch3 Albedo	float	Derived narrowband albedo value at 0.86 μm	grid (xsize, ysize)
Ch5 Albedo	float	Derived narrowband albedo value at 1.61 μm	grid (xsize, ysize)
Ch6 Albedo	float	Derived narrowband albedo value at 2.26 μm	grid (xsize, ysize)
Shortwave Albedo	float	Derived broadband albedo value at 0.4-3.0 μm	grid (xsize, ysize)
Albedo QF	char	Quality flag for each pixel, indicating the general retrieval quality	grid (xsize, ysize)
Albedo PQI	char	Product Quality Information for each pixel, indicating additional diagnostic information	grid (xsize, ysize)

Table 3.10. Outputs of the ABI albedo algorithm online mode: BRF

Name	Type	Description	Dimension
Ch1 BRF	float	Derived bidirectional reflectance value at 0.47 μm	grid (xsize, ysize)
Ch2 BRF	float	Derived bidirectional reflectance value at 0.64 μm	grid (xsize, ysize)
Ch3 BRF	float	Derived bidirectional reflectance value at 0.86 μm	grid (xsize, ysize)
Ch5 BRF	float	Derived bidirectional reflectance value at 1.61 μm	grid (xsize, ysize)
Ch6 BRF	float	Derived bidirectional reflectance value at 2.26 μm	grid (xsize, ysize)
BRF QF	char	Quality flag for each pixel, indicating the general retrieval quality	grid (xsize, ysize)
BRF PQI	char	Product Quality Information for each pixel, indicating additional diagnostic information	grid (xsize, ysize)

Correspondingly, we also have three groups of Quality Flag (QF) and Product Quality Information (PQI) information. One is for the intermediate BRDF parameter products, the second group is for albedo products, and the third group is for reflectance products. QF is a mandatory quality information required by GSP. The three groups of QF are defined in Tables 3.11-13.

Table 3.11. QF definition of ABI intermediate BRDF parameter products

Bit	Name	Value
0	Overall quality	0=good, 1 = bad or missing
1	Land mask	0=land, 1=water
2	Number of clear sky observations	0=sufficient, 1=insufficient
3	Convergence flag	0=good, 1=bad
4	Empty	Reserved for future usage
5		
6		
7		

Table 3.12. QF definition of ABI LSA products

Bit	Name	Value
0	Overall quality	0=good, 1 = bad or missing
1	Land mask	0=land, 1=water
2	Cloud	0=clear, 1=cloud
3	BRDF	0=good BRDF, 1= bad or missing BRDF
4	LZA	0= LZA <=70 degrees, 1 = LZA > 70 degrees
5	Empty	Reserved for future usage
6		
7		

Table 3.13. QF definition of ABI BRF products

Bit	Name	Value
0	Overall quality	0=good, 1 = bad
1	Land mask	0=land, 1=water
2	Cloud	0=clear, 1=cloud
3	LZA	0= LZA <=70 degrees, 1 = LZA > 70 degrees

4	BRDF	0= good BRDF, 1= bad or missing BRDF
5	AOD	0=AOD is good, 1=No AOD or AOD is bad
6	Empty	Reserved for future usage
7		

PQI contains additional quality information. The definitions of the three PQIs are given in Tables 3.14-16, respectively.

Table 3.14. PQI definition of ABI intermediate BRDF parameter products

Bit	Name	Value
0	Land mask	0=land, 1= water
1	BRDF inversion	00= full BRDF inversion, 01= low quality BRDF inversion (magnitude inversion only), 10=failure of BRDF inversion due to no enough clear sky observation, 11= failure of BRDF inversion due to other reasons.
2		
3	Data quality	00=high quality data, 01=data produced but with low quality, 10=no data
4		
5	Empty	Reserved for future usage
6		
7		

Table 3.15. PQI definition of ABI LSA products

Bit	Name	Value
0	Land mask	0=land, 1= water
1	Cloud mask	00=clear, 01=probably clear, 10=probably cloudy, 11=cloudy
2		
3	BRDF inversion	00= full BRDF inversion, 01= low quality BRDF inversion (magnitude inversion only), 10=failure of BRDF inversion due to no enough clear sky observation, 11= failure of BRDF inversion due to other reasons.
4		
5	Data quality	00=high quality data, 01=data produced but with low quality, 10=no data
6		
7	Empty	Reserved for future usage

Table 3.16. PQI Definition of ABI BRF products

Bit	Name	Value
0	Land mask	0=land, 1= water
1	Cloud mask	00=clear, 01=probably clear, 10=probably cloudy, 11=cloudy
2		
3	BRDF input	0=BRDF input, 1=Lambertian assumption
4	AOD input	0=AOD is available. 1 = no AOD
5	Data quality	00=high quality data, 01=data produced but with low quality, 10=no data
6		
7	Empty	Reserved for future usage

Besides the QF and PQI, each file of BRDF parameters, LSA and BRF products also comes with metadata information. The metadata information is given in Tables 3.17-19.

Table 3.17. Metadata of ABI intermediate BRDF parameter products

Metadata	Source	Definition
Date	common	Beginning and end dates of the product
Time	common	Beginning and end times of the product
Dimension	common	Number of rows, number of columns
Product Name	common	The ABI land surface BRDF parameter product
Satellite	common	GOES-R satellite name
Instrument	common	ABI
Version	common	Product version number
Data type	BRDF	Data type used to store BRDF parameters
Scale	BRDF	Scale used to stretch BRDF parameters
Offset	BRDF	Offset used to stretch BRDF parameters
Filling Value	BRDF	Value representing no data produced
Product Unit	BRDF	BRDF parameters are dimensionless
Compositing Period	BRDF	The compositing time period used to derive BRDF parameters.
QF categories	BRDF	Number of QF flag values
QF percentages	BRDF	Percent of retrievals with each QF flag value

Table 3.18. Metadata of ABI LSA products

Metadata	Source	Definition
Date	common	Beginning and end dates of the product
Time	common	Beginning and end times of the product
Dimension	common	Number of rows, number of columns
Product Name	common	The ABI land surface albedo product
Satellite	common	GOES-R satellite name
Instrument	common	ABI
Version	common	Product version number
Data type	LSA	Data type used to store albedo values
Scale	LSA	Scale used to stretch albedo
Offset	LSA	Offset used to stretch albedo
Filling Value	LSA	Value representing no data produced
Valid Range	LSA	Valid range of albedo values, 0-1
Product Unit	LSA	Albedo is dimensionless
Compositing Period	LSA	The compositing time period used to derive BRDF parameters.
Statistics	LSA	Maximums, minimums, means and standard deviations of albedos
QF categories	LSA	Number of QF flag values
QF percentages	LSA	Percent of retrievals with each QF flag value

Table 3.19. Metadata of ABI BRF products

Metadata	Source	Definition
Date	common	Beginning and end dates of the product
Time	common	Beginning and end times of the product
Dimension	common	Number of rows, number of columns
Product Name	common	The ABI land surface reflectance product
Satellite	common	GOES-R satellite name
Instrument	common	ABI
Version	common	Product version number
Data type	BRF	Data type used to store reflectance values
Scale	BRF	Scale used to stretch reflectance
Offset	BRF	Offset used to stretch reflectance
Filling Value	BRF	Value representing no data produced
Valid Range	BRF	Valid range of reflectance values, 0-2
Product Unit	BRF	Reflectance is dimensionless
Compositing Period	BRF	The compositing time period used to derive BRDF parameters.

Statistics	BRF	Maximums, minimums, means and standard deviations of reflectances
QF categories	BRF	Number of QA flag values
QF percentages	BRF	Percent of retrievals with each QF flag value

4 TEST DATA SETS AND OUTPUTS

The algorithm will be tested using three types of proxy data: MODIS, SEVIRI and the simulated ABI data.

4.1 Input Data Sets and Ground Measurements

4.1.1 Proxy Input Data

One characteristic of the ABI LSA algorithm is that it takes advantage of two features of ABI measurements -- high temporal refreshing rates and multi-spectral configuration -- to achieve the goal of retrieving atmospheric conditions and surface BRDFs simultaneously. However, no existing satellite sensors can provide ideal proxy data with such characteristics to facilitate our algorithm verification activities. We use both MODIS and MSG/SEVIRI data here. MODIS has similar spectral configuration (seven bands for the land application) to ABI. However, MODIS is a polarorbiting sensor and maps the Earth surface only twice in most cases even if we combine both Terra and Aqua satellites. The current geostationary satellites (e.g. GOES, MSG) have high refreshing rate, but none of them has as many bands as ABI. Table 4.1 lists the visible and near infrared bands of the MSG/SEVIRI, MODIS and ABI.

Table 4.1. Comparison of SEVIRI, MODIS and ABI reflective bands.

Sensor	Temporal resolution	Channel No.	Wavelength Center (μm)	Bandwidth (μm)
ABI	15min	1	0.47	0.45 – 0.49
		2	0.64	0.59 – 0.69
		3	0.86	0.85 – 0.88
		5	1.61	1.58 – 1.64
		6	2.26	2.23 – 2.28
SEVIRI	15min	2	0.635	0.56 - 0.71
		3	0.81	0.74 - 0.88
		4	1.64	1.50 - 1.78
MODIS	Polar-orbiting	1	0.646	0.62-0.67
		2	0.857	0.84-0.88
		3	0.466	0.46-0.48
		4	0.554	0.55-0.57
		5	1.242	1.23-1.25
		6	1.629	1.63-1.65

		7	2.114	2.11-2.16
--	--	---	-------	-----------

4.1.1.1 Simulated Data

Since none of existing satellite sensors can provide proxy data with both the high temporal resolution and multiple-channels as ABI data, simulation will be the only way to test our algorithm's ability to handle ABI data before GOES-R is launched. We use Qin et al. (2001)'s formulation of atmospheric radiative transfer to simulate TOA signals and assure the simulated TOA signals have the following properties:

- Use the ABI band configuration and band response functions.
- Bear the realistic observing geometry and refreshing rate of ABI.
- Consider the couple between the atmosphere and surface BRDF.

In order to simulate the signals received by the spaceborne sensors, both the surface properties and atmospheric parameters are needed in addition to the sensor response functions. We use the BRDF parameters from the MODIS albedo products as the input of surface properties. The AOD data come from the field measurements at SURFRAD sites as the atmospheric conditions. Similar to the solar radiation, AOD is also measured every 3 minutes using visible Multi-Filter Rotating Shadowband Radiometers (MFRSR). SURFRAD AOD measurements include five bands (415.0, 501.6, 613.5, 671.7 and 867.5nm). However, the 6S simulation requires the AOD input at 550nm. We calculate this value using the Angstrom Equation:

$$\tau_{\lambda} = \beta\lambda^{-\alpha}$$

where λ is the wavelength, τ_{λ} is the AOD at λ . α and β are coefficients, which are obtained through the linear regression if AOD measurements at three bands are valid. An example of such time series of AOD at 550nm is given in Figure 4.1.

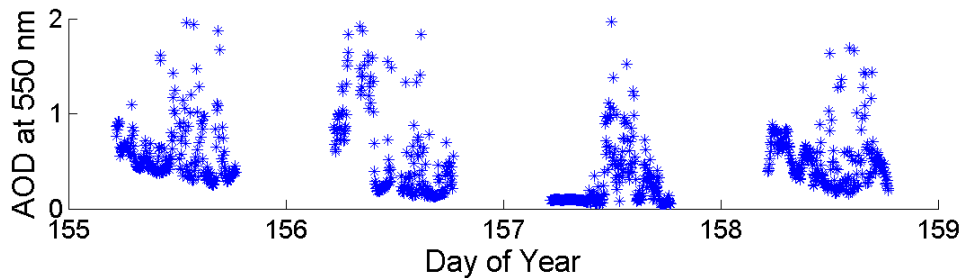


Figure 4.1 An example input of AOD time series at the Bondville site. The AODs at 550nm are calculated from AODs at other bands using the Angstrom Equation.

4.1.1.2 MODIS Data

We carried out two types of validation activities using MODIS as proxy data. First, we extracted the point data over the SURFRAD and AmeriFlux sites for the whole year of 2005 and directly compare our retrievals with field measurements. We also generated a time series of ten days' MODIS data as proxy data to test the operational ability of the

LSA algorithm over 2D images. MODIS is a polar-orbiting sensor. The L1B MODIS swath cannot be directly used to stack the time series because each of these swaths has different spatial coverage. We have to project all the MODIS L1B swath data to a common map projection. MODIS radiance, geolocation data and MODIS cloud mask, water vapor and AOD products, covering the MODIS tile H11V04 and the period of May 1 to 10, 2005, are downloaded. We used the MODIS Reprojection Tool to project these data sets to MODIS's sinusoidal map projection. The projected data will be passed to AIT and used as the test dataset. The detailed information of these datasets is given in Table 4.2.

Table 4.2. Detailed information of MODIS test data sets

Dataset Name	Description	File names*	Dimension
MOD02	MODIS/Terra TOA Radiance	H10V4.AYYYYDDD.HHMM.hdf	1200*1200
MOD03	MODIS/Terra Geolocation	H10V4.AYYYYDDD.HHMM.hdf	1200*1200
MYD02	MODIS/Aqua TOA Radiance	H10V4.BYYYYDDD.HHMM.hdf	1200*1200
MYD03	MODIS/Aqua Geolocation	H10V4.BYYYYDDD.HHMM.hdf	1200*1200
MOD04	MODIS/Terra Aerosol	MOD04.H10V4.AYYYYDDD.HHMM.hdf	120*120
MYD04	MODIS/Aqua Aerosol	MYD04.H10V4.AYYYYDDD.HHMM.hdf	120*120
MOD07	MODIS/Terra Water Vapor	MOD07.H10V4.AYYYYDDD.HHMM.hdf	240*240
MYD07	MODIS/Aqua Water Vapor	MYD07.H10V4.AYYYYDDD.HHMM.hdf	240*240
MOD35	MODIS/Terra Cloud Mask	MOD35_L2.H10V4.AYYYYDDD.HHMM.hdf	1200*1200
MYD35	MODIS/Aqua Cloud Mask	MYD35_L2.H10V4.AYYYYDDD.HHMM.hdf	1200*1200
MCD43	MODIS albedo climatology	MCD43.H10V4.AYYYYDDD.HHMM.hdf	1200*1200

* YYYY = year, DDD = day, HH=hours and MM = minutes. All times are in UTC

4.1.2 Ground Measurements

Albedo measurements over SURFRAD and AmeriFlux networks are used in our validation (Table 4.3 and Table 4.4). Albedo is calculated as the ratio of outgoing and incoming solar irradiance. Incoming and outgoing shortwave radiation is measured every 3 minutes at SURFRAD sites using the Eppley Precision Spectral Pyranometers (PSP), which are calibrated annually. The spatial and temporal representation of field measurements and satellite retrievals are usually different. The averages of albedo over 30 minutes are used to compare with instantaneous albedo retrieved by our algorithm to

mitigate the mismatch. The MODIS albedo products have a temporal resolution of 16 days. The corresponding averages of field measurements are used to match MODIS data sets. Different from the measurements at SURFRAD, field data at the AmeriFlux sites contain only the radiation in the visible spectrum. So the validation results at these AmeriFlux sites are only for visible albedo.

Table 4.3. Information of SURFRAD Stations

Site No.	Site Location	Latitude	Longitude	Surface types
1	Bondville, IL	40.05	-88.37	Crop
2	Desert Rock, NV	36.63	-116.02	Open shrub
3	Fort Peck, MT	48.31	-105.10	Grass
4	Goodwin Creek, MS	34.25	-89.87	Deciduous Forest
5	Pennsylvania State University, PA	40.72	-77.93	Mixed Forest
6	Sioux Falls, SD	43.73	-96.62	Forest

Table 4.4. Information of AmeriFlux Stations

Site No.	Site Location	Latitude	Longitude
1	Fort Peck	48.31	-105.10
2	Fermi(Prairie)	41.84	-88.24
3	Mead(Irrigated)	41.17	-96.48
4	Mead(Rain fed)	41.18	-96.44

4.2 Output from Proxy Data

4.2.1 Output from Simulated Data

More validation work using simulated ABI data is ongoing. Preliminary results show our retrieval could capture the BRDF distribution well under a variety of atmospheric and surface settings. One example is given in Figure 4.2. Although the two BRDF data sets come from different empirical models, they have similar reflectance distribution shapes. However, due to the feature of the BRDF model we use in the albedo algorithm, a hot-spot effect is noticeable in our retrieved BRDF distribution.

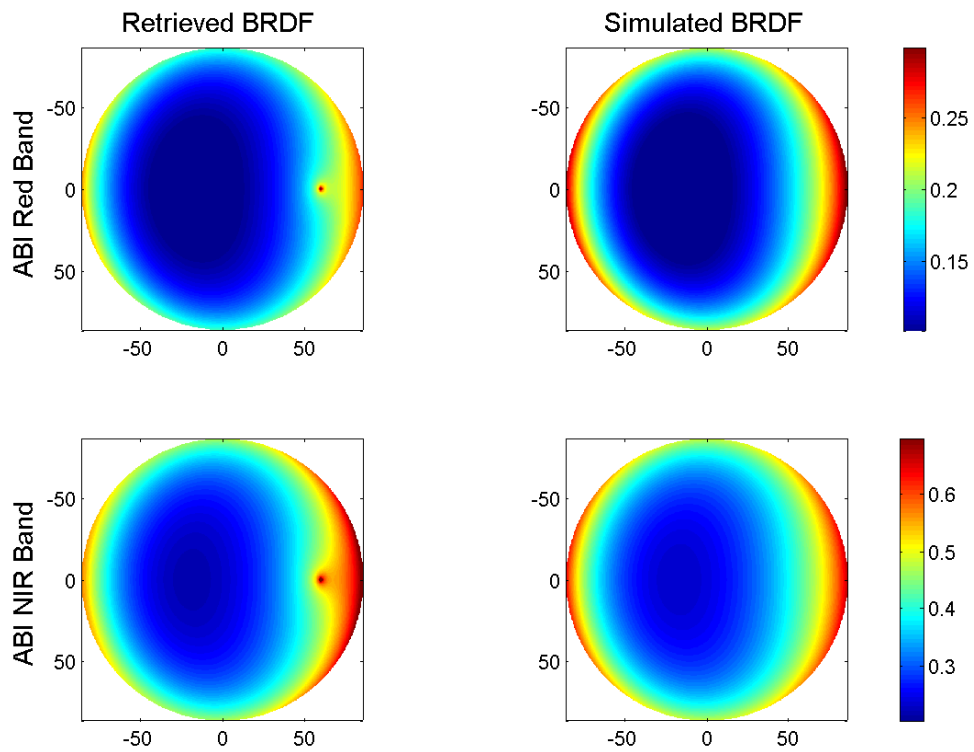


Figure 4.2 The retrieved BRDF and the actual BRDF used in the simulation at ABI red and near infrared bands.

4.2.2 Output from 2D MODIS Data

The LSA algorithm was carried out on these time series of 2D images to generate albedo maps at each observation time. The retrieved blacksky albedo on May 1st, 2005 around 48.3°N, 102.8°W is shown in Figure 4.3. The MODIS blacksky albedo for the same time and location is also shown. Our estimation captures a similar spatial pattern to MODIS data but has slight underestimation (Figure 4.4).

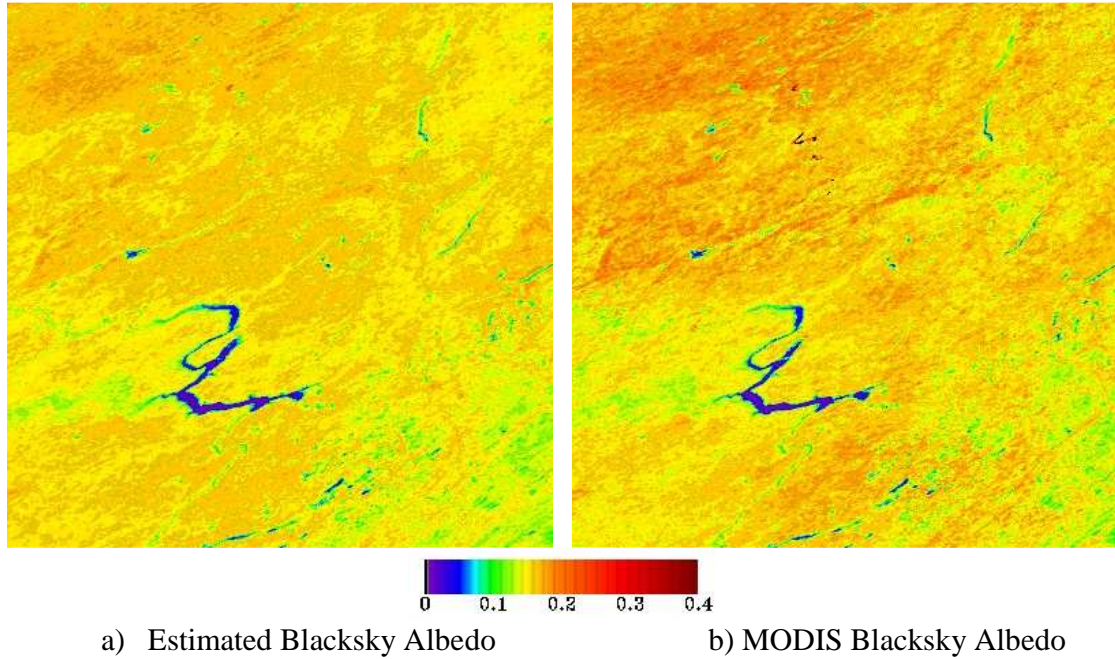


Figure 4.3 The blacksky albedo maps on May 1st, 2005 around 48.3°N, 102.8°W.

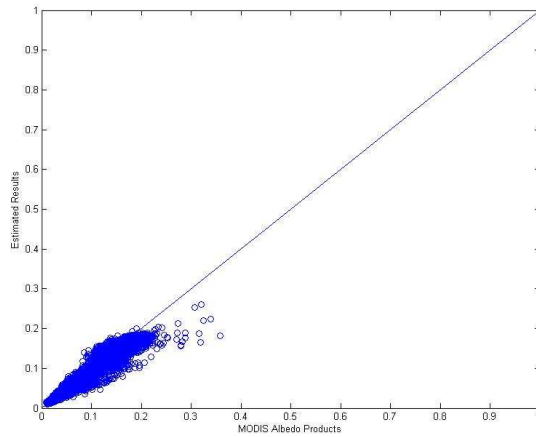


Figure 4.4 Comparison between our retrieved albedo and MODIS albedo.

4.2.3 Output from MODIS Data over Field Sites

The direct validation results of our retrieved albedo values at SURFRAD are shown both in time series (Figure 4.5) and scattering plots (Figure 4.6). Generally, the retrieved albedo values match well with field measurements. For the non-snow cases (Desert Rock and Goodwin Creek), the Root Mean Square Errors (RMSE) are quite small, although the R^2 values are rather low due to the small range of albedo variations. The undetected

clouds may be the main cause of albedo overestimation in Desert Rock. At Goodwin Creek, both our estimations and MODIS products are slightly lower than field measurements. This may come from the inaccurate representations of aerosol types. Both our retrievals and MODIS albedo data can reasonably represent the seasonal snow albedo over Bondville, Fort Peck and Sioux Falls. Our retrieval algorithm requires shorter compositing window, which makes it possible to better capture the rapid snowfall/melting processes when ABI data are available.

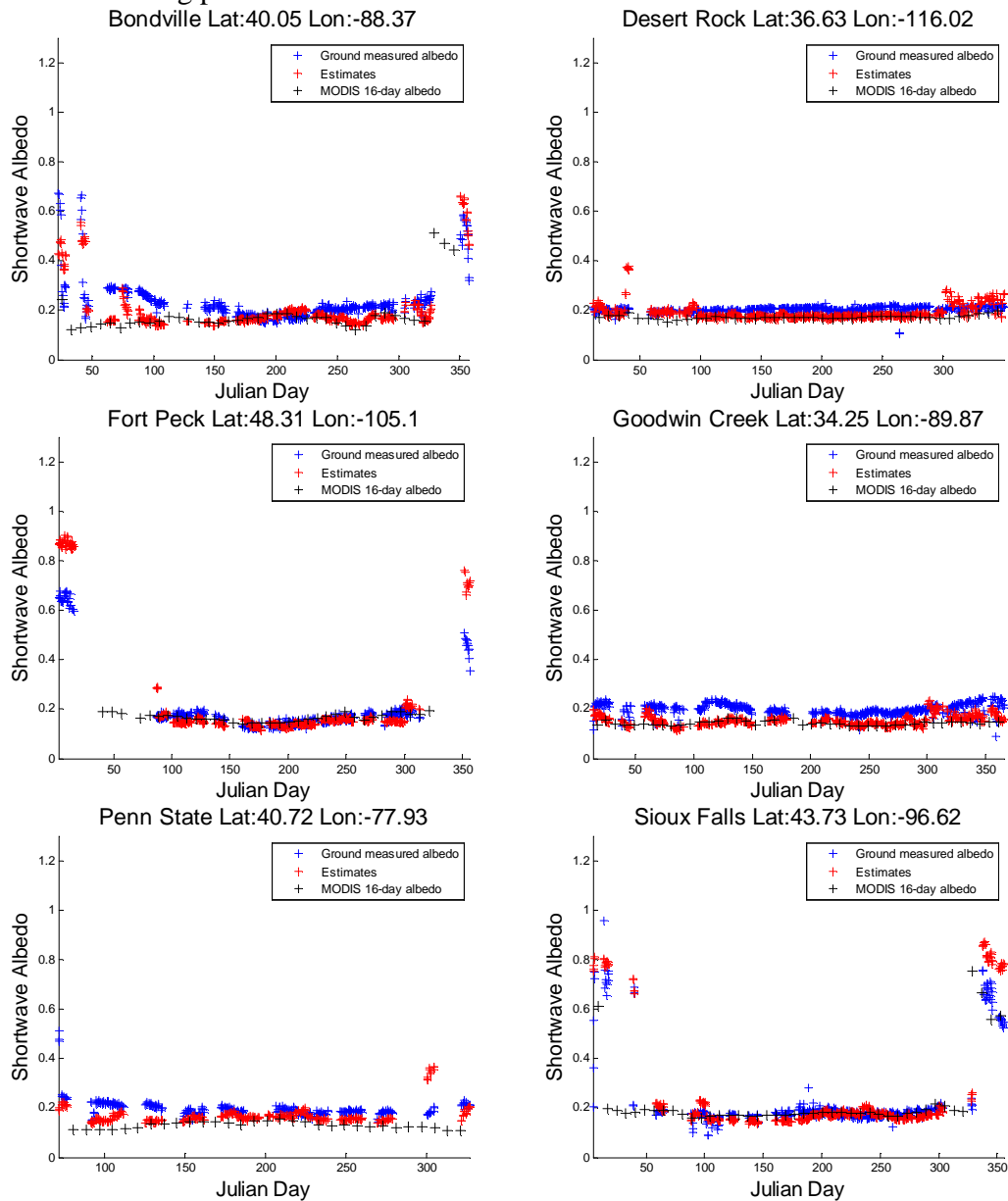


Figure 4.5. Time series of validation results of the LSA algorithm using MODIS as proxy data in 2005 over six SURFRAD sites.

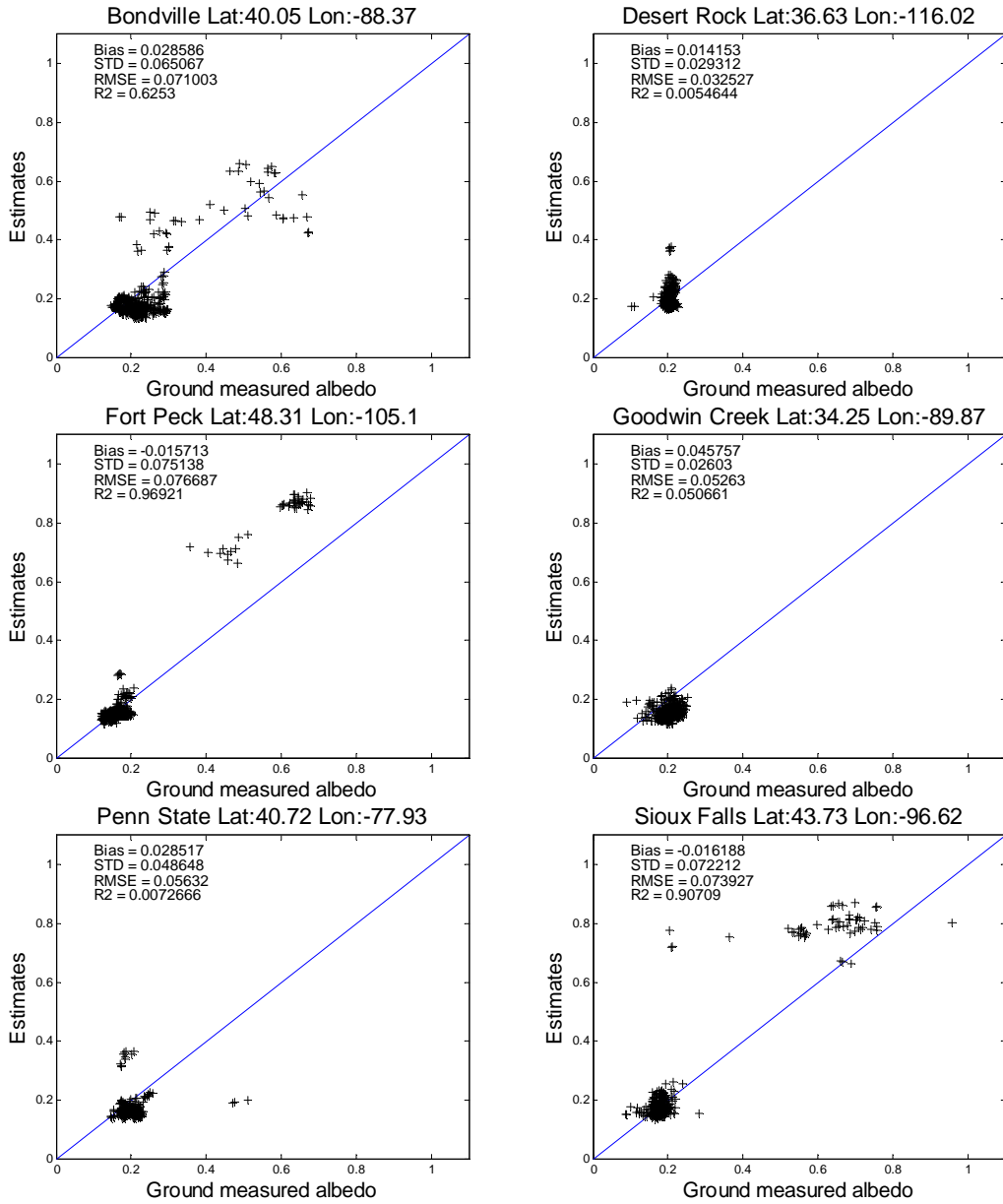


Figure 4.6 Scattering plots of our retrieved albedo over SURFRAD

The validation results at four AmeriFlux sites are shown in Figures 4.7-9. The results shown here are visible albedo because only irradiances in the visible spectrum are measured at these sites. Similar to the results at SURFRAD, our algorithm can capture the annual curves of albedo, but produces larger errors for rapidly changing surfaces. Overall, the RMSE of our retrievals at these four sites is much smaller than that of MODIS products (Figure 4.9).

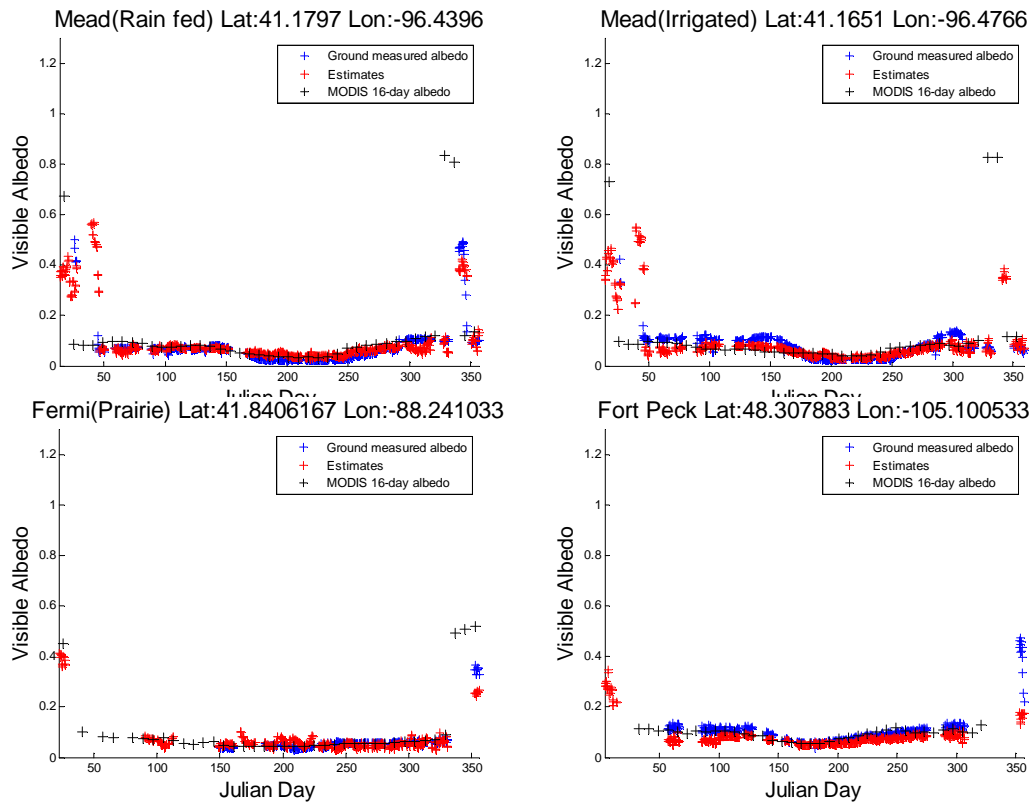


Figure 4.7. Time series of validation results of the LSA algorithm using MODIS as proxy data in 2005 over four AmeriFlux sites.

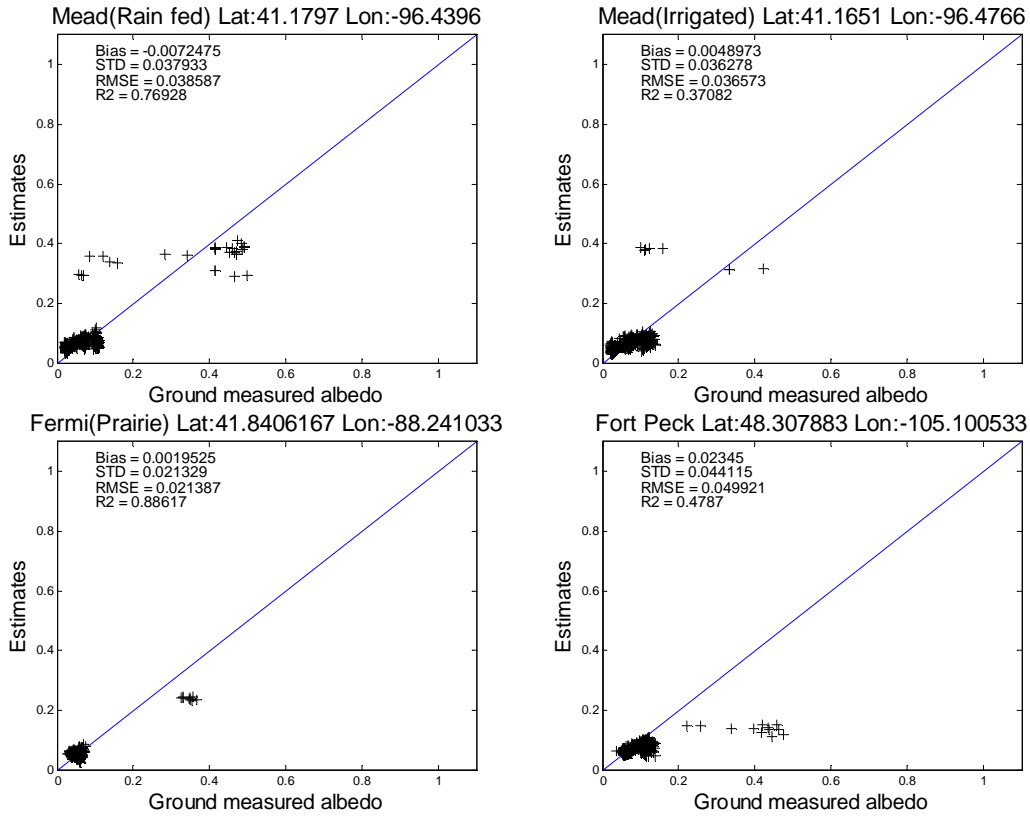


Figure 4.8 Scattering plots of our retrieved albedo over four AmeriFlux sites

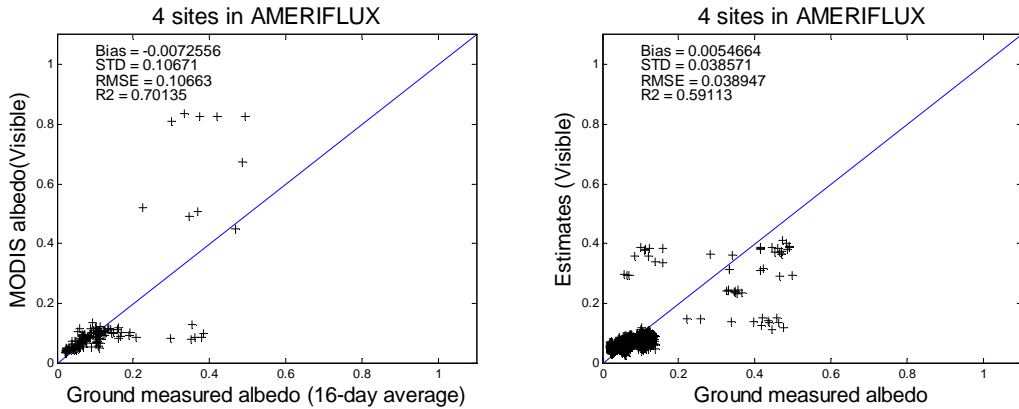


Figure 4.9 The overall quality of our retrieved albedo and MODIS albedo products using all the four AmeriFlux sites data over year 2005.

4.2.4 Summary of Estimate Accuracy and Precision

The validation results of the six SURFRAD sites are given in Figure 4.10. Compared with MODIS albedo products, our algorithm performs slightly better in terms of bias, RMSE and R^2 . We should also notice that our algorithm produces much more data than MODIS, because our products are instantaneous while MODIS products are 16-day

composite values. The listed accuracy requirement for ABI albedo is 0.08 albedo unit and the error (RMSE) of our retrievals is 0.01. In terms of RMSE (precision), we achieve a value of 0.06 while the F&PS requirement is 10% (Table 4.5). For the real ABI data, we expect even higher accuracy, since the ABI data have a temporal resolution of 15 minutes, providing sufficient data within a shorter time period, which is extremely important for the cases of rapidly changing surface properties, such as transitions between snowfall and snow melting.

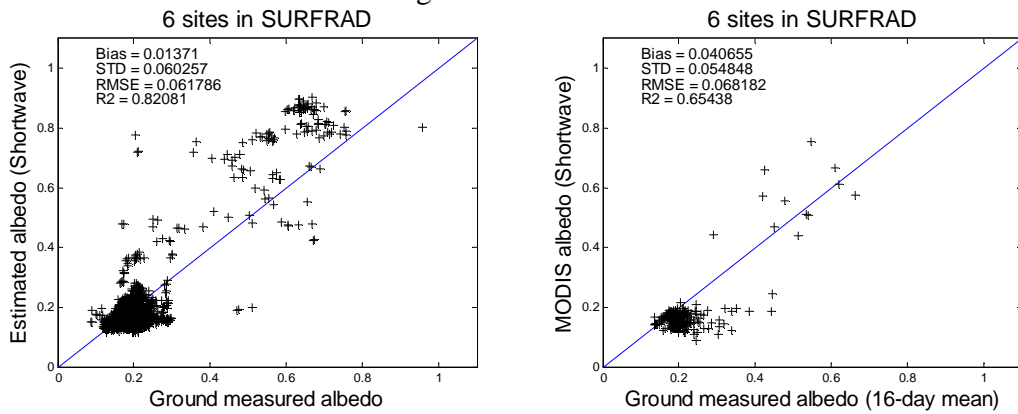


Figure 4.10 The overall quality of our retrieved albedo and MODIS albedo products using all the six sites data over year 2005.

Table 4.5. Information of AmeriFlux Stations

	Our algorithm	MODIS Products	F&PS Requirement
Accuracy(Bias)	0.01	0.04	0.08
Precision(RMSE)	0.06	0.07	10%
R^2	0.82	0.65	N/A

5 PRACTICAL CONSIDERATIONS

5.1 Numerical Computation Considerations

Accurate retrieval of albedo requires reliable acquisition of atmospheric parameters. Forward running of atmospheric radiative transfer model is time-consuming and not suitable for operational retrieval of albedo. Instead, the LSA algorithm pre-runs the atmospheric radiative transfer at some given conditions and stores the parameters into the LUTs to save computational time.

The current version of the LSA algorithm includes an optimization process. To speed up the iterative process, we may have to limit the number of iterations or adjust the iteration convergence criteria.

5.2 Programming and Procedural Considerations

The LSA algorithm is purely a pixel-by-pixel algorithm. However, it requires a time series of clear-sky observations to achieve enough information to inverse BRDF models. Given the data volume of full disk albedo products, it is inefficient to gather a stack time series data over all pixels at each ABI scanning time. Given that the BRDF parameters do not vary greatly over a short period of time, we use the pre-calculated BRDF parameters from the previous day to save computational time. In order to achieve this, we divide our algorithm into two parts, online and offline modes, respectively.

5.3 Quality Assessment and Diagnostics

The retrieval process of albedo will be monitored and the retrieval quality will be assessed. A set of quality flags will be generated with the albedo product for retrieval diagnostics. These flags will indicate the retrieval conditions, including the land/non-land mask, clear/cloudy sky. These flags also indicates the data quality (are clear sky observations sufficient? Is the data quality of AOD reliable? Is a full inversion of BRDF successful?). The detailed information is documented in Section 3.6.

5.4 Exception Handling

The LSA algorithm checks for conditions where the albedo retrieval cannot be performed. These conditions include the failure of sensors, such as saturated channels or missing values. They also include the conditions when continuous clouds are present so that there are no enough clear-sky observations. Under these circumstances, we will:

- Provide filling value for albedo when no enough clear sky input is available.
- Provide filling value for surface reflectance when the observation is cloudy.

5.5 Algorithm Validation

A summary of our previous validation results has been given in Section 4. In order to quantify the retrieval errors and improve the inversion algorithm, we need to carry out more extensive validation work before and after launch of the GOES-R satellite. Albedo is continuously measured by several surface measurement networks, such as Atmospheric Radiation Measurement at the Southern Great Plains, SURFRAD, and Ameriflux projects. Albedo measurements at more than a hundred sites are available for pre-launch and post-launch validation. We have conducted albedo validation extensively during recent years (Chen et al. 2008; Liang et al. 2002; Liang et al. 2005b), and will continue this activity for the ABI albedo product over more surface types.

6 ASSUMPTIONS AND LIMITATIONS

The following sections describe the assumptions in developing and estimating the performance of the current version of ABI LSA algorithm. The limitations and potential algorithm improvement are also discussed.

6.1 Performance

The following assumptions have been made in developing and estimating the performance of the ABI LSA algorithm:

- Surface BRDF is the revised linear kernel model with three coefficients.
- Surface anisotropy is constant within days through a moving window and can be represented by the linear kernel model.
- The reciprocity principle is valid at ABI resolutions.

6.2 Assumed Sensor Performance

The ABI LSA algorithm requires a time series of clear sky TOA reflectance inputs. The number of clear sky observations within a short time period will influence the retrieval quality of LSA and corresponding land surface reflectance by-products. Additionally, the algorithm relies on the cloud mask product to distinguish clear-sky observations from cloud sky observations. The retrieval accuracy also depends on the quality of cloud mask.

6.3 Algorithm Improvement

The introduction of prior knowledge such as the aerosol types, BRDF and albedo climatologies will improve the retrieval quality of LSA and land surface reflectance. Currently, we use the multiyear's mean and variance of MODIS albedo products as one of the constraints in our optimization code. We are currently working on analyzing more existing satellite albedo and BRDF products and in an effort to incorporate as much background knowledge as possible.

7 REFERENCES

- Chen, Y.M., Liang, S., Wang, J., Kim, H.Y., & Martonchik, J.V. (2008). Validation of MISR land surface broadband albedo. *International Journal of Remote Sensing*, 29, 6971-6983
- Christopher, S.A., Zhang, J., Holben, B.N., & Yang, S.K. (2002). GOES-8 and NOAA-14 AVHRR retrieval of smoke aerosol optical thickness during SCAR-B. *International Journal of Remote Sensing*, 23, 4931-4944
- Deuze, J.L., Breon, F.M., Devaux, C., Goloub, P., Herman, M., Lafrance, B., Maignan, F., Marchand, A., Nadal, F., Perry, G., & Tanre, D. (2001). Remote sensing of aerosols over land surfaces from POLDER-ADEOS-1 polarized measurements. *Journal of Geophysical Research-Atmospheres*, 106, 4913-4926
- Diner, D.J., Martonchik, J.V., Kahn, R.A., Pinty, B., Gobron, N., Nelson, D.L., & Holben, B.N. (2005). Using angular and spectral shape similarity constraints to improve MISR aerosol and surface retrievals over land. *Remote Sensing of Environment*, 94, 155-171
- Duan, Q.Y., Gupta, V.K., & Sorooshian, S. (1993). Shuffled complex evolution approach for effective and efficient global minimization. *Journal of Optimization Theory and Applications*, 76, 501-521
- Duan, Q.Y., Sorooshian, S., & Gupta, V. (1992). Effective and efficient global optimization for conceptual rainfall-runoff models. *Water Resources Research*, 28, 1015-1031
- Fang, H.L., Liang, S.L., Kim, H.Y., Townshend, J.R., Schaaf, C.L., Strahler, A.H., & Dickinson, R.E. (2007). Developing a spatially continuous 1 km surface albedo data set over North America from Terra MODIS products. *Journal of Geophysical Research-Atmospheres*, 112
- Govaerts, Y.M., Wagner, S., Lattanzio, A., & Watts, P. (2010). Joint retrieval of surface reflectance and aerosol optical depth from MSG/SEVIRI observations with an optimal estimation approach: 1. Theory. *Journal of Geophysical Research-Atmospheres*, 115
- Hauser, A., Oesch, D., Foppa, N., & Wunderle, S. (2005). NOAA AVHRR derived aerosol optical depth over land. *Journal of Geophysical Research-Atmospheres*, 110
- Kaufman, Y.J., Tanre, D., Remer, L.A., Vermote, E.F., Chu, A., & Holben, B.N. (1997). Operational remote sensing of tropospheric aerosol over land from EOS moderate

resolution imaging spectroradiometer. *Journal of Geophysical Research-Atmospheres*, 102, 17051-17067

Liang, S., Yu, Y., & Defelice, T.P. (2005a). VIIRS narrowband to broadband land surface albedo conversion: formula and validation. *International Journal of Remote Sensing*, 26, 1019-1025

Liang, S.L. (2001). Narrowband to broadband conversions of land surface albedo I Algorithms. *Remote Sensing of Environment*, 76, 213-238

Liang, S.L. (2004). *Quantitative remote sensing of land surfaces*. Hoboken, New Jersey: John Wiley & Sons, Inc

Liang, S.L., FallahAdl, H., Kalluri, S., JaJa, J., Kaufman, Y.J., & Townshend, J.R.G. (1997). An operational atmospheric correction algorithm for Landsat Thematic Mapper imagery over the land. *Journal of Geophysical Research-Atmospheres*, 102, 17173-17186

Liang, S.L., Fang, H.L., Chen, M.Z., Shuey, C.J., Walthall, C., Daughtry, C., Morissette, J., Schaaf, C., & Strahler, A. (2002). Validating MODIS land surface reflectance and albedo products: methods and preliminary results. *Remote Sensing of Environment*, 83, 149-162

Liang, S.L., Shuey, C.J., Russ, A.L., Fang, H.L., Chen, M.Z., Walthall, C.L., Daughtry, C.S.T., & Hunt, R. (2003). Narrowband to broadband conversions of land surface albedo: II. Validation. *Remote Sensing of Environment*, 84, 25-41

Liang, S.L., Stroeve, J., & Box, J.E. (2005b). Mapping daily snow/ice shortwave broadband albedo from Moderate Resolution Imaging Spectroradiometer (MODIS): The improved direct retrieval algorithm and validation with Greenland in situ measurement. *Journal of Geophysical Research-Atmospheres*, 110

Liang, S.L., Zhong, B., & Fang, H.L. (2006). Improved estimation of aerosol optical depth from MODIS imagery over land surfaces. *Remote Sensing of Environment*, 104, 416-425

Maignan, F., Breon, F.M., & Lacaze, R. (2004). Bidirectional reflectance of Earth targets: Evaluation of analytical models using a large set of spaceborne measurements with emphasis on the Hot Spot. *Remote Sensing of Environment*, 90, 210-220

NOAA (2009). GOES-R Series Ground Segment Project Functional and Performance Specification. In

North, P.R.J. (2002). Estimation of aerosol opacity and land surface bidirectional reflectance from ATSR-2 dual-angle imagery: Operational method and validation. *Journal of Geophysical Research-Atmospheres*, 107

Orgill, J.F., & Hollands, K.G.T. (1977). Correlation equation for hourly diffuse radiation on a horizontal surface. *Solar Energy*, 19, 357-359

Pinty, B., Roveda, F., Verstraete, M.M., Gobron, N., Govaerts, Y., Martonchik, J.V., Diner, D.J., & Kahn, R.A. (2000a). Surface albedo retrieval from Meteosat - 1. Theory. *Journal of Geophysical Research-Atmospheres*, 105, 18099-18112

Pinty, B., Roveda, F., Verstraete, M.M., Gobron, N., Govaerts, Y., Martonchik, J.V., Diner, D.J., & Kahn, R.A. (2000b). Surface albedo retrieval from Meteosat - 2. Applications. *Journal of Geophysical Research-Atmospheres*, 105, 18113-18134

Qin, W.H., Herman, J.R., & Ahmad, Z. (2001). A fast, accurate algorithm to account for non-Lambertian surface effects on TOA radiance. *Journal of Geophysical Research-Atmospheres*, 106, 22671-22684

Remer, L.A., Kaufman, Y.J., Tanre, D., Mattoo, S., Chu, D.A., Martins, J.V., Li, R.R., Ichoku, C., Levy, R.C., Kleidman, R.G., Eck, T.F., Vermote, E., & Holben, B.N. (2005). The MODIS aerosol algorithm, products, and validation. *Journal of the Atmospheric Sciences*, 62, 947-973

Schaaf, C., Martonchik, J., Pinty, B., Govaerts, Y., Gao, F., Lattanzio, A., Liu, J., Strahler, A., & Taberner, M. (2008). Retrieval of Surface Albedo from Satellite Sensors. In S. Liang (Ed.), *Advances in Land Remote Sensing: System, Modeling, Inversion and Application* (pp. 219-243). New York: Springer

Schaaf, C.B., Gao, F., Strahler, A.H., Lucht, W., Li, X.W., Tsang, T., Strugnell, N.C., Zhang, X.Y., Jin, Y.F., Muller, J.P., Lewis, P., Barnsley, M., Hobson, P., Disney, M., Roberts, G., Dunderdale, M., Doll, C., d'Entremont, R.P., Hu, B.X., Liang, S.L., Privette, J.L., & Roy, D. (2002). First operational BRDF, albedo nadir reflectance products from MODIS. *Remote Sensing of Environment*, 83, 135-148

Vermote, E.F., El Saleous, N.Z., & Justice, C.O. (2002). Atmospheric correction of MODIS data in the visible to middle infrared: first results. *Remote Sensing of Environment*, 83, 97-111

Wagner, S.C., Govaerts, Y.M., & Lattanzio, A. (2010). Joint retrieval of surface reflectance and aerosol optical depth from MSG/SEVIRI observations with an optimal estimation approach: 2. Implementation and evaluation. *Journal of Geophysical Research-Atmospheres*, 115

Wang, D., & Liang, S. (2010a). Improving LAI Mapping by Integrating MODIS and CYCLOPES LAI Products Using Optimal Interpolation. *Remote Sensing of Environment*, Submitted

Wang, D., & Liang, S. (2010b). Integrating MODIS and CYCLOPES LAI using EOF. *IEEE Transactions on Geoscience and Remote Sensing*, Submitted

Wang, D., & Liang, S. (2010c). Using multiresolution tree to integrate MODIS and MISR-L3 LAI products (Abstract). In, *2010 IGRASS*

Wang, K., Liang, S., Wang, D., & Zheng, T. (2008). Simultaneous estimation of surface photosynthetically active radiation and albedo from GOES. In, *Proceedings of IEEE International Geoscience and Remote Sensing Symposium 2008* (pp. 311-314). Boston, MA, USA

Zhong, B., Liang, S., & Holben, B. (2007). Validating a new algorithm for estimating aerosol optical depths over land from MODIS imagery. *International Journal of Remote Sensing*, 28, 4207-4214